University of Alberta

Association of Model Compounds of Asphaltenes in Organic Solutions

By

Amir Hassan Soleimani Salim

A thesis submitted to the Faculty of Graduate Studies and Research
in partial fulfillment of the requirements for the degree of

Master of Science

in

Chemical Engineering

Department of Chemical and Materials Engineering

ABSTRACT

The self-association properties of two model compounds of asphaltene, 2,6-bis[2-(pyren-1-yl)ethyl]pyridine (PyPPy, C41H29N) and 2,6-bis[2-(phenanthren-9-yl)ethyl]pyridine (PhPPh, $C_{37}H_{29}N$), were studied in deuterated chloroform and deuterated methylene chloride. ^{1}H NMR spectroscopy titration experiments showed that both compounds undergo changes in conformation in solution as a function of solvent, concentration, and water concentration. At low concentrations, below 0.1 mM in chloroform, these compounds gave ^{1}H NMR chemical shifts consistent with intra-molecular interaction, likely due to a folding conformation. At concentrations above 10 mM the ^{1}H NMR chemical shifts were consistent with inter-molecular interactions due to aggregation. Results of spin- lattice relaxation time (T_1) measurement and diffusion-ordered spectroscopy (DOSY) experiments are consistent with existence of two conformations at low and high concentrations. The addition of water promotes aggregation of these model compounds even at low concentrations of 10^{-5} M, likely via hydrogen bonds between the pyridyl nitrogens and water. Temperature had no effect on aggregation of the model compounds in the range -60°C to +55°C.

ACKNOWLEDGEMENTS

Contents

LIST OF TABLES

LIST OF FIGURES

LIST OF SCHEMES

NOMENCLATURE

ABBREVIATIONS

PhPPh	2,6-bis[2-(phenanthren-9-yl)ethyl]pyridine ($C_{37}H_{29}N$) or 2,6-phenanthrene-pyridine
PyPPy	2,6-bis[2-(pyren-1-yl)ethyl]pyridine ($C_{41}H_{29}N$) or 2,6-pyrene-pyridine
NMR	Nuclear magnetic resonance
^{1}H NMR	Proton nuclear magnetic resonance
DOSY	Diffusion-Ordered Spectroscopy
ASTM	American Society for Testing and Materials
VPO	Vapor Pressure Osmometry
MALDI	Matrix–Assisted Laser Desorption / Ionization
HCCA	α-Cyano-4-hydroxycinnamic acid

SYMBOLS

T	Temperature
R	Universal gas constant
T_1	Spin-lattice or longitudinal relaxation time
K	Equilibrium constant
ΔH	Enthalpy
ΔG	Gibbs free energy
C	Concentration
t	Time
[D]	Concentration of folded conformation
$[D_2]$	Concentration of aggregated conformation
D	Diffusion coefficient

1. INTRODUCTION

The asphaltene fraction of petroleum includes the largest, densest, and most polar compounds (Sheu, 2002). These compounds tend to aggregate and form a colloidal phase even at low concentrations in crude oil, over a wide range of temperatures (Akbarzadeh et al., 2005). Understanding how the asphaltene molecules self associate to build aggregates, then form flocs, and finally precipitate, is essential in linking the onset of precipitation in heavy oil and bitumen processing to the underlying molecular structure and behavior. Operating problems such as deposition, precipitation plugging, fouling on heated surfaces and catalyst deactivation may all be alleviated by a better understanding of asphaltene behavior (Absi-Halabi et al., 1991; Akbarzadeh et al., 2004). Even in the reservoir, asphaltenes can block the pores of reservoir rocks (Yudin and Anisimov, 2007) and cause a reduction in oil flow (Agrawala and Yarranton, 2001).

The asphaltene fraction of an actual crude oil is much too complex to define the detailed intermolecular interactions in solution. One approach is to conduct well-controlled experiments on defined solutions of components. Dr. Xiaoli Tan (X Tan, personal communication, 2011) already investigated a set of homologous series of model compounds of asphaltene in deuterated chloroform (Table 1.1) and interestingly observed that model compounds without nitrogen inside the molecule don't show aggregation behavior in organic solution. These results confirm that association behaviour of model compounds is not only due to

aromatic groups, and even in the case of large aromatic groups there is no association.

	Association Behaviour in ^{1}H NMR titration
	NO
	NO
	NO
	NO
	YES
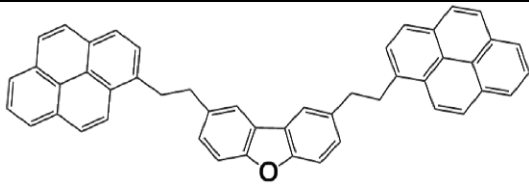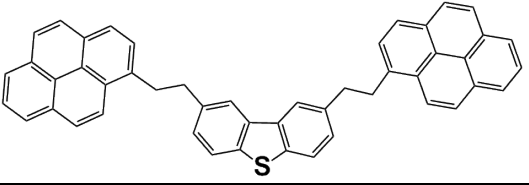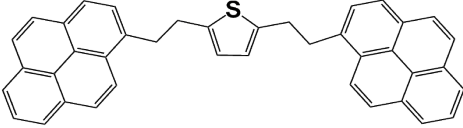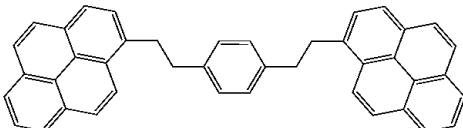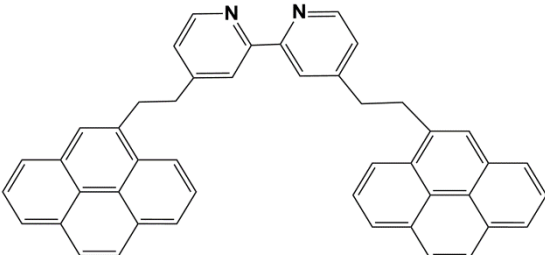
Table 1.1. Results of aggregation behaviour of model compound of asphaltenes without nitrogen in deuterated chloroform.

Tan et al. (Tan et al., 2008) showed that a model compound containing a bipyridine group with two nitrogen atoms gave association in solution, and that this association was senstitive to water. Components with a single nitrogen atom are more abundant in petroleum, therefore, the objective of this project was to investigate pyridine derivatives. In this research, self-association of two model compounds of asphaltene, 2,6-bis[2-(pyren-1-yl)ethyl]pyridine (PyPPy, $C_{41}H_{29}N$) and 2,6-bis[2-(phenanthren-9-yl)ethyl]pyridine (PhPPh, $C_{37}H_{29}N$), were studied in deuterated chloroform and methylene chloride using ^{1}H NMR spectroscopy titration, spin–lattice relaxation time (T_1) measurement, and diffusion-ordered spectroscopy (DOSY) experiments.

(a)

(b)
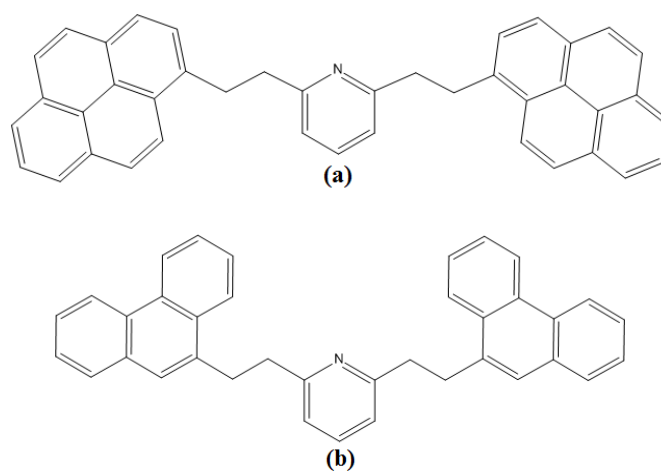
Scheme 1.1 Chemical structures of (a) 2,6-bis[2-(pyren-1-yl)ethyl]pyridine or 2,6-pyrene-pyridine (PyPPy), (b) 2,6-bis[2-(phenanthren-9-yl)ethyl]pyridine or 2,6-phenanthrene-pyridine (PhPPh)

The thesis is organized in three chapters, including this introduction and the abstract. The first chapter gives background on the relevant literature related to

the asphaltenes and self association of this fraction. In this chapter, a brief overview of the asphaltenes, including their definition, main properties and effects of them on self association of asphaltenes, is presented. In addition, it includes background about nuclear magnetic resonance spectroscopy (NMR) as the main method which used in this thesis.

The second chapter contains the materials, methods and conditions were chosen to investigate self association of model compounds of asphaltenes.

The third chapter reports results of self association of PyPPy and PhPPh in deuterated chloroform and methylene chloride. The results of the nuclear magnetic resonance spectroscopy (NMR) techniques indicate that both compounds show intra-molecular interaction or folding conformation at concentrations below 0.1 mM and give aggregation by inter-molecular interactions above 10 mM. The conformations arising from intra- and inter-molecular interactions co-exist in the range of 0.1-10 mM.

2. Literature background

2.1. Asphaltene

Petroleum crude oils are complex mixtures of millions of different compounds (Hughey et al., 2002). Asphaltenes are the heaviest and most polar compounds in crude oils, and are defined as the solubility class which is obtained from crude oil by fractionation using solvents (Fossen et al., 2011). As prepared in the laboratory by solvent precipitation, asphaltenes are brownish-black powdery materials precipitated by addition of light n-alkanes to crude oils or bitumens (Speight, 2004). A further specification is that asphaltenes are soluble in aromatic solvents (Speight, 2004). This least-soluble fraction of petroleum is also characterized by high aromaticity, molecular weight and polarity (Freund et al., 2007). These properties make the asphaltene precipitation from petroleum feedstock a complex process that is affected by a number of factors, such as solvents, ratio of solvents, time and etc. (Freund et al., 2007). Therefore, with different methods of precipitation and solvents, the properties and behaviour of asphaltene from a given crude oil will change.

Asphaltenes have a high amount of metals and heteroatoms, relative to the whole crude oil, and are very reactive during processes (Spiecker et al., 2003; Gawrys et al., 2006; Speight, 2007). They can decrease activity and also life of catalysis.

In the refinery many different solvents over a range of dilution and temperatures may be used for precipitation of asphaltenes for the preparation of

asphalts, such as paraffins, isoparaffins, straight run naphtha or other non-aromatic solvents (Mitchell and Speight, 1973). The research studies in laboratories demonstrate that the solvent type, dilution degree, temperature, and contact time are the major factors that influence the yield and properties of the asphaltenes from a given crude oil (Mitchell and Speight, 1973; Speight, 2006).

The amount of asphaltenes precipitated by different solvents such as normal paraffins, isoparaffins, cycloparaffins, terminal olefins, aromatics, and blends of different ratios of benzene and n-pentane correlates linearly with the solubility parameter of these solvents and blends (Mitchell and Speight, 1973). The solubility parameter is a measure of the solvent power, or the energy of the solution, to overcome the association forces of the solute (Hildebrand, 1919; Hildebrand et al., 1970). Therefore, aromatic solvents, with their higher dispersion forces, have high cohesive energy and the paraffins are less dense and have a lower cohesive energy density (Mitchell and Speight, 1973). Although, chemical composition of asphaltenes is almost same for different solvent blendssome properties of precipitated asphaltenes such as apparent molecular weight are different (Alboudwarej et al., 2002). Even when using the same solvent, the yield of asphaltenes is affected by the degree of dilution of bitumen or other petroleum materials in solvent (Alboudwarej et al., 2002). As the ratio of the precipitating solvent increases, keeping other factors constant, the asphaltenes yield increases until it reaches a plateau when the solvent ratio is above circa 25 mL/g of asphaltenes (Alboudwarej et al., 2002). The type of interactions responsible for inducing precipitation is petroleum–dependent and in some crude the polar and

H–bonding interactions are more important and in other crudes dispersion forces are likely more significant (Gawrys et al., 2006).

Yield of precipitated asphaltenes increases as the temperature increases due to the decrease in the solubility parameter of the low molecular weight solvents, such as pentane, as the temperature increases (Mitchell and Speight, 1973).

2.2. Properties of the Petroleum Asphaltenes

In this section some properties of asphaltenes that are relevant to the aggregation behavior of asphlatenes will be outlined.

2.2.1. Elemental Composition

The asphaltenes are composed of C, H, N, S, O, Ni, and V (Siskin et al., 2006). For example, weight percent of C, H, S, N, and O in the asphaltenes from Alberta heavy oils and bitumen are 80.06 -86.61, 6.93 -8.45, 3.47 -8.21, 0.94 - 2.82, and 0.44 -2.61, respectively (Speight, 2006). The Ni and V are more concentrated in the VR and the asphaltenes, compared to the rest of the bitumen. For example, the concentrations of Ni and V in Athabasca bitumen are 65 and 196 ppm, respectively, but the n–pentane asphaltenes from this bitumen contained Ni and V at 312 and 710 ppm, respectively.

2.2.2. Aromaticity

The H/C ratio of the n-C7 (n-heptane) asphaltenes from Alberta heavy oils and bitumen are in the range of 0.98–1.26, which is less than the ratio for the source oils, ~1.5 H/C, from which these asphaltenes were obtained (Speight, 2006). This low H/C ratio is indicative of the high aromaticity of the asphaltenes and the carbon aromatic content of asphaltenes that were derived from different sources were in the range of 36–50%, and up to 55% for Athabasca n- C7 asphaltenes (Asprino et al., 2005; Siskin et al., 2006). Silva et al. (Silva & Seidl, 2004) with using NMR technique reported 58.8- 58.6 percent % of aromatic carbons for the asphaltenes obtained from different vacuum residues according to the IP-143/96 method (IP Standards for Petroleum and Its Products, 1960).

	Asphaltene
% of aromatic carbons	58.8 -58.6
% of saturated carbons	41.2 -41.4
% of aromatic carbons bonded to alkyl branches	10.4 -9.5
% of aromatic carbons bonded to hydrogen	15.4 -14.7

Table 2.1. Properties of asphaltenes obtained by 1H and 13C NMR (Silva & Seidl, 2004).

2.2.3. Density and Viscosity

The density and viscosity of the asphaltenes is higher than the heavy oils and bitumen and show the heavy nature of this fraction and the challenges in handling the asphaltenes after separation from the feedstocks and during transportation and upgrading processes. For Athabasca bitumen the density of the saturates, aromatics, resins, and asphaltenes from is 900, 1003, 1058, and 1192 kg/m3, respectively (Akbarzadeh et al., 2004).

The asphaltenes show an extremely viscous nature when they are in the melt state, such that the n-C7 Athabasca asphaltenes are almost 100 times more viscous than the whole VR (Asprino et al., 2005).

2.2.4. Molecular Weight

Yarranton et al. (Yarranton, Alboudwarej, & Jakher, 2000) showed that MW in toluene is a measure of aggregation and even stronger solvents can fail to fully disperse asphaltenes molecules. Generally, for a homologous series of compounds, the boiling point increases with increasing the molecular weight (Boduszynski, 1987). But for complex mixtures like VR or the asphaltenes this rule is not valid as it has been shown that compounds with similar molar masses have a broad boiling point range and, on the contrary, a specific and narrow boiling point cut consists of a wide range of molar masses (Boduszynski, 1987). A wide range of molar masses have been reported for asphaltenes, from 500- 3000 Da (Groenzin and Mullins, 1999, 2000; Strausz et al., 2002; Groenzin et al., 2003; Akbarzadeh et al., 2004; Mullins et al., 2008; Mullins, 2010). The main reason for the different results for the molecular weights of the asphaltenes obtained from different characterization method, sometimes the same method at different conditions, is due to the complexity and associative behavior of the asphaltene molecules (Strausz et al., 2008). Also, due to the use of methods that cannot possibly give proper average estimates for a complex mixture. For example, for Athabasca asphaltenes dissolved in o-dichlorobenzene at 120 °C, vapor pressure osmometry (VPO) gave a molar mass of about 4000 g/mol for the aggregated asphaltenes (Strausz et al., 2002). On the other hand, reported a VPO value for Athabasca asphaltenes reported as 7900 g/mol in toluene, which was associated with the self–association of asphaltenes, and therefore the molar mass results

depended on both the temperature and the solvent (Akbarzadeh et al., 2004). Also, Fluorescence depolarization supported the claim of smaller molecular weights in the range of 500–1000 Da (Groenzin and Mullins, 1999, 2000; Groenzin et al., 2003; Mullins et al., 2008; Mullins, 2010). However, this method was not supported by proper control experiments to show the ability of the method to measure average molecular weights in complex mixtures of polyfunctional molecules such as asphaltenes (Strausz et al., 2008).

Application of field desorption mass spectroscopy to VR derived asphaltenes gave an average molecular weight of 1238 Da, with the range extending from ~300–3000 Da (Qian et al., 2007). All of these methods lacked appropriate calibration standard methods to verify the ability of the method to properly measure molecular weight of complex polyfunctional molecules. The main reasons for the uncertainty in measuring the molecular weight are different size and composition of asphaltene molecules and the self association behavior of asphaltens which affect accuracy of measurements (Strausz et al., 2008).

2.2.5. Molecular Structure

The molecular structure of petroleum asphaltenes is the key to understanding the origin and behaviour of these components (Pelet et al., 1986; di Primio R et al., 2000; Freund et al., 2007). Due to the complexity of the asphaltenes, there are still many debates on a representative chemical structure, even after reaching a consensus on the approximate range of molecular weights of the asphaltenes. The main two structures suggested for the asphaltenes are the "archipelago" compounds; consist of alkyl bridged aromatic and cycloalkyl groups linked together mainly with alkyl carbon bridges and the "continental" compounds which composed of highly alkylated condensed polycyclic aromatic compounds (Pelet et al., 1986; Groenzin and Mullins, 2000; Strausz and Lown, 2003; Mullins, 2010).

The archipelago model was suggested by Strausz and co–workers after observing that large amounts of mono-, di-, tri-, and up to pentacyclic aromatic species were released by mild thermolysis of the asphaltenes (Ignasiak et al., 1977; Rubinstein and Strausz, 1979; Rubinstein et al., 1979). Thermal degradation studies of Alberta asphaltenes resulted in identification of many structural units which are consistent to be in alkylated homologous series (Strausz et al., 1992). In addition, the selective oxidation of the aromatic rings, using ruthenium ion–catalyzed oxidation (RICO), by which the aromatic carbons are removed as CO_2 and the saturated carbons are left unchanged, showed the abundance of alkyl chains and bridges in the asphaltenes (Strausz et al., 1992; Artok et al., 1999).

Karimi et al. (Karimi et al., 2011) obtained quantitative data for the existence of bridged structures in the asphaltenes by using thin film pyrolysis. In this method the rapid thermal cracking of the asphaltenes at 500 °C generated gases, liquid, and coke with over 91% recovery. The use of a thin film minimized the secondary reaction of cracked fragments by maximizing the release of products into the vapor phase where they were immediately quenched. Analysis of the liquid products from this method confirmed the existence of mono– up to tetra–, aromatic and naphthenic rings, paraffins, thiophenes, benzothiophenes, sulfides, and nitrogen bearing molecules (Karimi et al., 2011). Similar yields of cyclic and aromatic fragment groups were obtained from a range of crude oils from Canada, China, Mexico, Saudi Arabia, and Venezuela.

Therefore all of these studies support a structural motif for a significant mass fraction of asphaltenes consisting of polycyclic aromatic and aliphatic groups connected by short alkyl bridges, like an archipelago of islands. The work of Karimi et al., 2011 showed that Strausz's earlier structural work on Athabasca could be generalized to a much wider range of crude oils.

Figure 2.1 shows a structure of an archipelago model of Sheremata et al. (Sheremata et al., 2004). Although the structures suggested by Sheremata et al. (Sheremata et al., 2004) and Strausz et al. (Strausz et al., 1992) have molecular weights of 4000–6000 Da, which is higher than the current accepted range in the literatures, smaller molecules can be represented as portions of this model while preserving the structural aspects of asphaltenes.
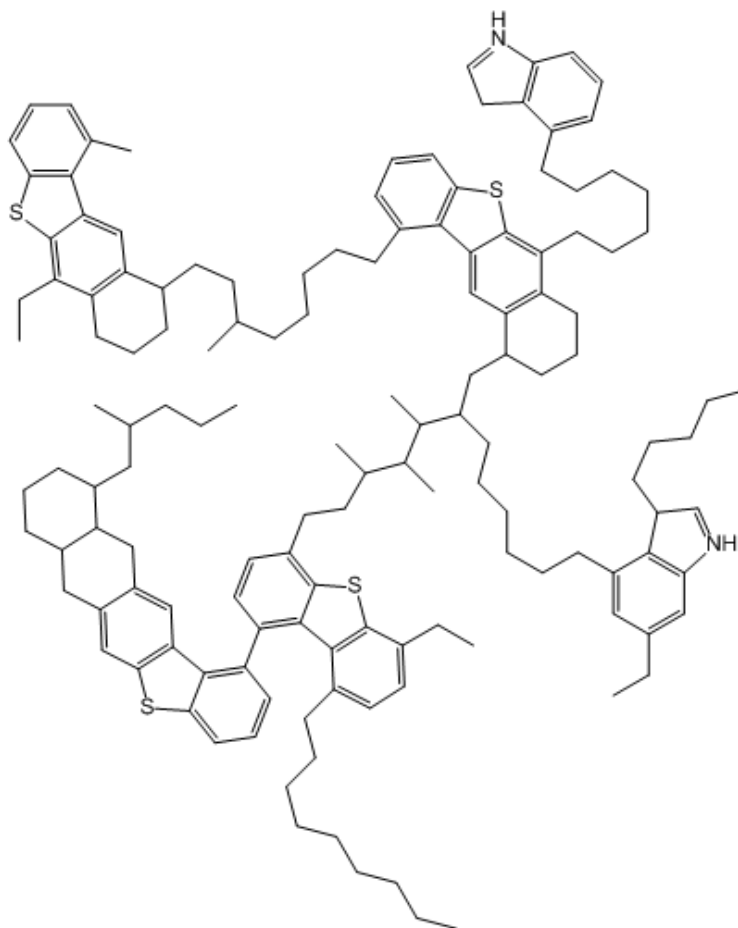
Figure 2.1. archipelago model of Sheremata et al. (Sheremata et al., 2004) with reduced molecular weight to fit the ~500–2000 Da range.

The continental, island, or pericondensed structural model consists of highly condensed polyalkylated aromatic compounds, some with fused saturated rings (Pfeiffer and Saal, 1940; Dickie and Yen, 1967; Groenzin and Mullins, 2000). Figure 2.2 shows one representative island model structures suggested by Mullins (Mullins, 2010).
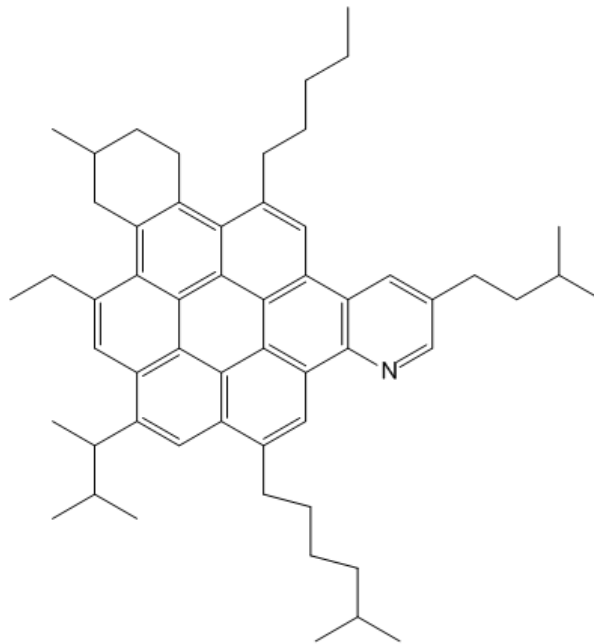
Figure 2.2. Island model structure for asphaltenes suggested by Mullins (Mullins, 2010).

The arguments for the presence of the condensed alkyl aromatic structures depend on either fluorescence spectroscopy (Groenzin and Mullins, 2000), which cannot be used to determine "average" or most probable structures in a complex mixture of components (Strausz et al., 2008), or mass spectrometry experiments that lacked proper calibration by proper reference compounds. Large ring structures, such as vanadyl and nickel porphyrins, are present in the heavy fractions of petroleum, but they do not appear to dominate in commonly processed heavy oils and bitumens.

Isolation of single molecules and probing their chemical structure from the complex mixture of the asphaltenes is not possible, but all the results from accurately calibrated instruments, the quantitative evidence of pendant groups, the

structure of kerogen, and the behavior of asphaltenes during processing (Gray, 2003), support the archipelago motif as the dominant chemical structure of asphaltenes.

2.2.6. Self–Association

Asphaltenes self associate in solutions over a wide range of concentrations and temperatures (Akbarzadeh et al., 2005).

The associative properties of asphaltenes in solvents and crude oils has been studied by many researchers by different methods such as small angle X-ray and neutron scattering (SANS) (Sheu et al., 1992; Gawrys et al., 2003; Tanaka et al., 2003), vapor pressure osmometry (VPO)(Yarranton et al., 2000; Agrawala and Yarranton, 2001), isothermal titration calorimetry (ITC) (Merino-Garcia and Andersen, 2003), gel permeation chromatography (GPC) (Seidl et al., 2004), high quality factor (high-Q) ultrasonics (Andreatta et al., 2005), molecular simulations (Murgich and Aray, 1996; Murgich, 2003), and fluorescence depolarization (Groenzin and Mullins, 2000). Nevertheless, understanding the behavior of asphaltenes at the molecular level is challenging due to the high polydispersity and chemical diversity of this fraction. Due to this complexity, the mechanisms of self-association of asphaltenes are not well-understood(Sheu, 2002).

The stability of asphaltenes depends upon several factors including the solvent type, degree of dilution, pressure, and temperature (Buenrostro-Gonzalez et al., 2004; Espinat et al., 2004; Shaw and Zou, 2007).

According to island model (Dickie and Yen, 1967; Mullins, 2010), many researchers suggest that the main forces causes the asphaltene molecules to self associate together is predominantly π–π stacking (Dickie and Yen, 1967; Mullins, 2010). Many references also suggest, however, that strong specific forces, such as

polar and stacking interactions involving heteroatoms and aromatic moieties, promote asphaltene aggregation while weaker nonspecific dispersion forces control asphaltene precipitation (Buckley, 1996, 1999; Gutiérrez et al., 2001; Spiecker et al., 2003).

One effective method to investigate the molecular and self association behaviors of asphaltenes is to synthesize and study model compounds of asphaltenes that mimic the chemical functional groups and physical characteristics of this solubility class (Akbarzadeh et al., 2005; Tan et al., 2008, 2009). Investigations of Some polynuclear aromatic hydrocarbons using pyrenyl and hexabenzocoronene suggested the importance of the large alkylated polynuclear aromatic hydrocarbons and oxygen-containing polar chains for self-association (Akbarzadeh et al., 2005; Rakotondradany et al., 2006). Akbarzadeh et.al (Akbarzadeh et al., 2005) suggested that polar functional groups will contribute to association behavior, even in strong solvents, at elevated temperature. Smaller aromatic groups in pyrene and alkyl-bridged dipyrene gave no association. Investigation of alkyl hexabenzocoronenes suggest that either larger aromatic groups or more alkyl side groups would be required to enhance association in solution (Ito et al., 2000), while formation of small bridged structures reduces the tendency to associate in solvents (Tchebotareva et al., 2003; Akbarzadeh et al., 2005).

Tan et. al (Tan et al., 2008, 2009), observed self association of different nitrogen bearing model compounds, according to archipelago model for asphaltene, on the basis of nuclear magnetic resonance, steady state fluorescence,

vapor pressure osmometry, solubility, and adsorption behavior studies. They suggested that this aggregation behavior was attributed to multiple π–π stacking interactions involving both pyrene rings and the bipyridine spacer and more favorable stacking at low temperatures.

Durand and coworkers (Durand et al., 2008, 2009, 2010) investigated association behavior of asphlatenes using nuclear magnetic resonance (NMR) and diffusion-ordered spectroscopy (DOSY). However, these data are full of doubts as the proton and carbon spectra and diffusion-ordered spectroscopy for the asphaltenes are crowded and overlapped because of the presence of numerous aromatic, naphthenic, and aliphatic functions in asphaltenes molecules. Therefore these techniques are not suitable to study real asphaltenes.

Recently, it is demonstrated by Gray et al. (Gray et al., 2011) that the π–π stacking is only a contributing factor, rather than the dominant one, in the aggregation of asphaltene molecules. Testing a model compound with 13-ring condensed aromatics, they showed that the π-π stacking of even very large aromatics is too weak in toluene solutions to account for aggregation of asphaltenes in highly dilute solution or at elevated temperature (Gray et al., 2011). Also, other properties of asphaltenes like strong adhesion to a wide range of surfaces (Xing et al., 2010), occlusion of components that are otherwise soluble, interactions with resins and surfactants (Wiehe and Jermansen, 2003; Pierre et al., 2004), formation of films at oil-water interfaces (Kumar et al., 2001; Zhang et al., 2005; Varadaraj and Brons, 2007) and formation of aggregates that are elastic under tension is not consistent with only aromatic stacking by electrostatic or van

der Waals forces, called π-π stacking (Gray et al., 2011). Gray et al. (Gray et al., 2011) argued that the strong association of asphaltene is affected by number of associative forces that act together in building a supramolecular assembly of the asphaltenes, such as acid–base interaction, hydrogen bonding, axial coordination by metal complexes, van der Waals forces, and π–π stacking (figure 2.3). Each of these interactions is relatively weak by itself, but according to principal of supramolecular chemistry, strongly associated structures arise from the cumulative effects of multiple weak interactions(Gray et al., 2011). These forces will form stable aggregates, which is consistent with the recent findings on the aggregate structure of the asphaltenes as open and flocculated polymer–like materials (Agrawala and Yarranton, 2001), and fit with archipelago model for asphaltene molecules that have multiple functional groups.
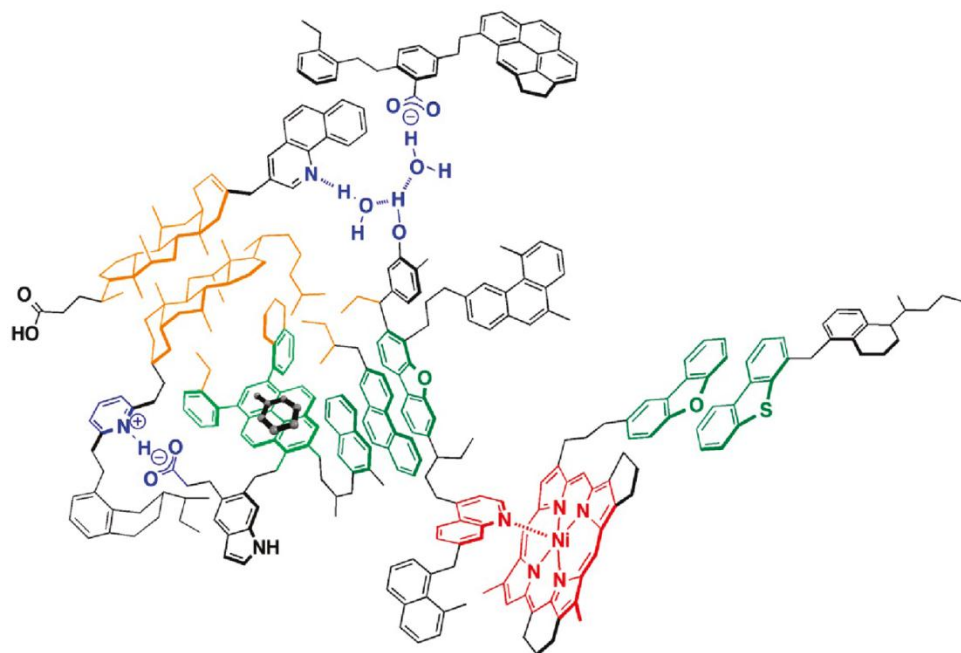
Figure 2.3. Representation of a supramolecular assembly suggested by Gray et. al (Gray et al., 2011) a representative asphaltene aggregate. Associations between molecules are color-coded in: acid-base interactions and hydrogen bonding (blue), metal coordination complex (red), a hydrophobic pocket (orange), π-π stacking (green)[1]

2.2.6.1. Role of water on aggregation of asphaltenes

Water plays a major role in the aggregation behavior of asphaltenes, because of participation in hydrogen-bonding formation (Tan et al., 2009). Andersen et al. (Andersen et al., 2001; Khvostichenko and Andersen, 2008) found that trace amounts of water in the solvent (<0.015%) had significant effects on the aggregation behavior of asphaltenes. Association because of water has been observed in asphaltene solutions by calorimetry (Merino-Garcia and Andersen, 2004) and with nitrogen bearing model compounds (Tan et al., 2009). Tan et al. (Tan et al., 2009) suggested that the O-H· · ·N hydrogen bonds between the pyridyl nitrogen and water were responsible for their aggregation at low concentrations, and that water enhanced the stability of aggregates by reinforcing π-π interactions via water bridged intermolecular H-bonding between the pyridyl nitrogen groups.

2.3. NMR spectroscopy

Nuclear magnetic resonance (NMR) spectroscopy is a powerful, molecular level technique that can give information on chemical functions and structural assemblies (Cardoza et al., 2004). There are many reports about different application of different NMR techniques for oil and petroleum fractions (Dickinson, 1980; Morris and Johnson, 1992; Pekerar et al., 1999; Merdrignac et al., 2006; Durand, Clemancey, Quoineaud, et al., 2008)

Nuclear magnetic resonance (NMR) uses the magnetic properties of nuclei to provide information about molecules (Friebolin, 2005; Levitt, 2008). NMR is a non destructive technique which can provide detailed information about structure, size, shape and dynamics of molecules (Abragam, 1983; Cardoza et al., 2004; Levitt, 2008). Nevertheless, the proton and carbon spectra and diffusion-ordered spectroscopy cannot be used for the establishment of a chemical structure of asphaltene because these are crowded and overlapped because of the presence of numerous aromatic, naphthenic, and aliphatic functions (Durand, Clemancey, Lancelin, Verstraete, Espinat, and Quoineaud, 2009a). As NMR spectroscopy is the main technique used in this study, the following section provides the basic theories and concepts of NMR spectroscopy. Application of NMR in this thesis is been limited to the 1H NMR spectroscopy, diffusion ordered spectroscopy (DOSY), spin-lattice or longitudinal relaxation time measurement experiments (T1 measurement), and transverse rotating-frame overhauser enhancement spectroscopy (2D-TROESY experiments).

2.3.1. Magnetic properties of nuclei

All atoms have a positively charged nucleus. These nuclei have magnetic properties causing the positive charge to circulate or spin around nucleus. This spin can produce a dipole along the axis of rotation. Therefore, nuclei with spin have angular momentum which can be explained as the spin quantum number (I) (Abragam, 1983; Levitt, 2008). Spin quantum number (I) of nuclei is dependent on the number of protons and neutrons, or in other words is dependent to atomic and mass number of atoms. Nuclei with both even mass and atomic number will have I=0. Nuclei with both odd mass and atomic number will have an integer spin, I=1, 2, etc). Nuclei with odd mass number and even atomic number will have a half integer spin, I= 1/2, 3/2, etc).

All nuclei with spin quantum number non equal to zero can produce a NMR signal and are considered as NMR visible nuclei. For example, 12C which has 6 protons and 6 neutrons in its nucleus has no net spin, since all spins are paired. Therefore, 12C does not produce any NMR signal. On the other hand, 13C which is another isotope of carbon, contains 6 protons and 7 neutrons and therefore has an unpaired spin which can produce a NMR signal (Abragam, 1983; Levitt, 2008). Table 2.1 lists some NMR-visible nuclei with their natural abundance.

Isotope	Spin (I)	Natural abundance (%)
1H	1/2	99.98
13C	1/2	1.07
15N	1/2	0.365
17O	5/2	0.037
19F	1/2	100
29Si	3/2	4.7
31P	1/2	100

Table 2.2: Some common NMR visible nuclei(Abragam, 1983; Levitt, 2008).

The magnetic dipole caused by inherent magnetic property of nuclei is proportional to spin quantum number(Abragam, 1983; Friebolin, 2005).

In case of thermal equilibrium and without an external magnetic field, the orientations of the nuclear spins are randomly distributed, but with an external magnetic field, the nuclear spins align. The possible orientations for nuclear spins alignments are described by the magnetic quantum number.

In case of I= 1/2, the magnetic quantum number is equal to 2, which means the nuclei has two different spin states in an applied magnetic field (i.e. +1/2 and -1/2). In the applied magnetic field, these two spins have different energy values which the spin +1/2 or ground state has lower energy than the spin -1/2 or excited state.

Therefore, higher magnetic field strength will cause a larger energy difference between two spin states.

Also, to produce a NMR signal, a little more nucleus must be present in the low energy state or ground state. The tendency of the NMR signal is correlated to the net difference in population of nuclei in the ground state and excited state. The net number of nuclei in ground state will increase with increasing overall energy differences between two spin states which is proportional to external magnetic field strength (Abragam, 1983).

2.3.2. NMR signal

A NMR signal is the result of adsorption of radio frequency (RF) pulse which is equal to energy difference (ΔE) between ground and excited states. If the external magnetic field was parallel to z-axis then the RF pulse is along x-axis and the signal is detected along y axis. When the RF is at the exact same frequency as ΔE, nuclei will be excited to the higher energy spin state from ground energy state. When the RF pulse is turned off, nuclei which have been excited to higher energy spin state, will slowly return to the ground state and will lose energy during this transmission. This process of nuclei going from the high energy state to the ground energy state is called relaxation, and the decay in energy called the free induction decay (FID) which is the NMR signal (Abragam, 1983).

2.3.3. Chemical shift

The positively charged nucleus of molecules is surrounded with an arrangement of electrons. The negative charge of electrons will cause a small magnetic field which shields the nucleus from the external magnetic field. A small variation in resonating frequency of nuclei will be caused by the shielding of nucleus. This change in the resonating frequency is expressed as the chemical shift. Therefore, the chemical shift a measure of the difference between external magnetic field and the magnetic field which is felt at nucleus (Abragam, 1983). Many parameters affect chemical shift, such as electron density, anisotropic-induced magnetic field effects and electronegativity (Abragam, 1983). More electron density of a nucleus will cause more shielding and results in lower chemical shift (Friebolin, 2005). Anisotropic-induced magnetic field effects are results of induced magnetic fields from circulating electrons around nuclei which can results a lower or higher chemical shifts (Friebolin, 2005). For example, the circulation of electrons in the aromatic orbitals of a benzene ring will create a magnetic field around the hydrogen nuclei which boost the effect of an external magnetic field and results in higher chemical shifts. Information about chemical and physical properties of nuclei and also its chemical environment can be extracted from chemical shift of a NMR signal (Friebolin, 2005).

The measurement of chemical shift for protons ($1H$) and $13C$ is taken relative to a reference compound which is usually tetramethylsilane (TMS) with

assigned chemical shift to zero. The range of chemical shits for 1H is narrow, 0-15 ppm, but for 13C it is between 0-200 ppm.

2.3.4. Relaxation

Relaxation measurements provide information about bonding, molecular motions, size and atomic distances between nuclei (Friebolin, 2005). There are two types of relaxation, longitudinal or spin-lattice relaxation and transverse or spin-spin relaxation. Longitudinal or spin-lattice relaxation, which is called T1, is the time for nuclei to lose energy to go from the excited state to the relaxed or ground state after RF pulsed is turned off which disturbed the equilibrium (Friebolin, 2005). Transverse or spin-spin relaxation, which is called T2, results from the transfer of energy between high energy state nuclei to nuclei of lower energy state which destroys phase coherence (Friebolin, 2005). In liquid state, T1 is bigger than T2 and they are both dependent on the system (Friebolin, 2005). In 1H NMR, the relaxation time of 1H is fairly short, on the order of a few seconds (Abragam, 1983).

Some parameters which affect T1 are molecular size, molecular shape, number of protons attached to nuclei (Abragam, 1983; Friebolin, 2005; Levitt, 2008). Usually T1-values decrease when the mobility of molecules decreases (Friebolin, 2005).

2.3.5. Two dimensional NMR spectroscopy (2D NMR)

2D NMR provides additional information such as nuclear connectivity information which cannot be obtained from 1D NMR. There many different 2D NMR techniques, and explaining all of them is beyond the scope of this thesis. Therefore, only a very brief explanation of two methods that we used in this thesis, DOSY and 2D-TROESY, and their advantages is discussed in the following sections.

2.3.5.1. Diffusion ordered spectroscopy (DOSY)

Diffusion ordered spectroscopy (DOSY) (Morris and Johnson, 1992; Johnson, 1999) was devised by Morris and Johnson (Morris and Johnson, 1992) as a high-resolution version of the pulsed field gradient stimulated echo nuclear magnetic resonance (PFGSE NMR) sequence. DOSY experiments allow analytical separation and identification of the mixture components (Durand, Clemancey, Lancelin, Verstraete, Espinat, and Quoineaud, 2009a). Also, it correlates chemical shifts with molecular diffusion or the mobility of each component. Therefore, the spectrum obtained from such an experiment is a two dimensional spectrum in which the x-axis is a conventional NMR spectrum (chemical shifts), and the y-axis is the diffusion coefficients (Friebolin, 2005). Parameters that affect diffusion coefficients include size, molecular weight, shape,

and aggregation status (Durand, Clemancey, Lancelin, Verstraete, Espinat, and Quoineaud, 2009a). The size and shape of compounds can be extracted from DOSY experiments.

Recently, DOSY experiments were used for asphaltenes by some researchers to provide information about aggregation of this solubility class (Cabrita & Berger, 2001; Durand et al., 2009a, 2009b, 2010; Durand, Clemancey, Lancelin, et al., 2008; Durand, Clemancey, Quoineaud, et al., 2008). Based on different diffusivity of different asphaltenes, Durand et. al (Durand et al., 2010) demonstrated that the chemical interactions of different asphaltenes from different sources are changed and, hence, they have different chemical structures. However, these data are not reliable as asphaltenes materials are a solubility class and a complex mixture of thousands of different molecules. Also, asphaltenes form nanoaggregates even at low concentrations and even strong solvents such as toluene cannot fully disperse asphaltenes aggregates. Therefore, From DOSY, it cannot be determined that the different diffusivity of different asphaltenes is related to different chemical composition, different size and extent of nanoaggregates, or chemical structure of ashplatenes.

2.3.5.2. Transverse Rotating-frame Overhauser Enhancement Spectroscopy (2D-TROESY)

This technique provides correlations based on through-space interactions of protons as opposed to correlations based on coupling interactions (Hwang and Shaka, 1992a, 1992b). This technique is usually used to provide structural information about the molecules and can provide information about which protons interact with each other (Abragam, 1983; Bross-Walch et al., 2005; Friebolin, 2005). There is no literature about application of this technique in asphaltene, but there many studies suggest that this technique can provide information about the protons which have interaction together from same molecule or two different molecule interaction of protons (Bradley et al., 1997; Auzély-Velty and Rinaudo, 2002; Bricout et al., 2012).

3. Materials and Methods

3.1. Materials

Two nitrogen-bearing model compounds for asphaltene were selected as highly simplified compounds to represent complex asphaltene species. The structures are shown in scheme 3.1. The compound 2,6-bis[2-(pyren-1-yl)ethyl]pyridine (PyPPy), consisted of two pyrene groups linked together by ethyl carbon bridges with a centre pyridine ring (scheme 3.1.a). The compound 2,6-bis[2-(phenanthren-9-yl)ethyl]pyridine (PhPPh), consisted of two phenanthrene groups linked together by ethyl carbon bridges with a centre pyridine ring (scheme 3.1.b). PhPPh was synthesized in the Department of Chemistry at University of Alberta by Dr. Stryker's group. PyPPy was synthesized in Department of Chemistry and Pharmacy at University of Erlangen-Nuremberg by Dr. Tykwinski's group. Briefly, the synthesis of these compounds required reaction of 1-ethynylpyrene or 1-ethynylphenanthrene with 2,6-dibromopyridine in THF and diisopropylamine to couple the ring groups together. The resulting ethyne bridges were then hydrogenated(Alshareef et al., 2011, 2012).

The purity of these compounds was checked using matrix-assisted laser desorption ionization (MALDI) (Jagtap and Ambre, 2005) with α-cyano-4-hydroxycinnamic (HCCA) as matrix. The impurity level of the model compounds was below the range of MALDI detection.
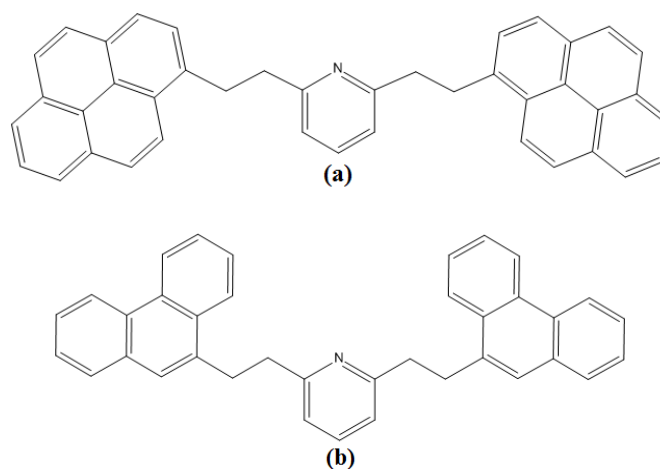
Scheme 3.1. Chemical structures of (a) 2,6-bis[2-(pyren-1-yl)ethyl]pyridine (PyPPy), (b) 2,6-bis[2-(phenanthren-9-yl)ethyl]pyridine (PhPPh)

Deuterated methylene chloride (CD_2Cl_2, 99.9 atom % D) was purchased from Sigma-Aldrich. For drying deuterated methylene chloride, we mixed 3Å molecular sieves (Caledon Laboratories Ltd, Ontario, CANADA), 20% mass/volume (m/v), and let the mixture stand for 48 hours inside a glove box (Williams and Lawton, 2010). Using this method, the water content in this laboratory-dried CD_2Cl_2 was below 0.001 wt %, which is below the detection limit of the Karl Fisher titration method(Eugen Scholz, 1984).

Water-saturated CD_2Cl_2 was obtained by mixing it in a separatory funnel with 50% (v/v) Ultrapure Millipore water (18.2 MΩ.cm) and separating the CD_2Cl_2 phase from the water phase after allowing the mixture to stand for a day. The amount of water in the solvent was determined with Karl-Fisher titration to be0.125 wt%.

Anhydrous deuterated chloroform ($CDCl_3$, 99.96 atom%D), sealed in ampoules, was purchased from Sigma-Aldrich. The amount of water in the

ampoules was quoted as being below 10 ppm. This solvent was not dried further. Tan et al. (Tan et al., 2009) had found previously that this level of moisture did not force aggregation in solution.

Deuterated chloroform ($CDCl_3$, 99.8 atom % D, Sigma-Aldrich) was used to make water-saturated deuterated chloroform. The water-saturated $CDCl_3$ was obtained by mixing it in a separatory funnel with 50% (v/v) Ultrapure Millipore water (18.2 MΩ.cm) and separating the $CDCl_3$ phase from the water phase after allowing the mixture to stand for a day. Acid wash deuterated chloroform was produce by mixing it in a separatory funnel with 50% (v/v) 1 N solution of HCl in Ultrapure Millipore water (18.2 MΩ.cm) and separating the $CDCl_3$ phase after allowing the mixture to stand for a day. Base wash deuterated chloroform were produced by mixing it in a separatory funnel with 50% (v/v) 1 N solution of KOH in Ultrapure Millipore water (18.2 MΩ.cm) and separating the $CDCl_3$ phase after allowing the mixture to stand for a day. All of the dried and water saturated solvents were sealed and stored in a glove box under inert condition of nitrogen to avoid any contamination and moisture effects.

All of the samples of PyPPy and PhPPh in deuterated chloroform and deuterated methylene chloride were prepared freshly just before each experiments to avoid effect of moisture or photo-oxidation on the samples.

3.2. Nuclear magnetic resonance spectroscopic analysis

The proton nuclear magnetic resonance (^{1}H NMR) spectroscopic chemical shifts of the protons for solutions of PyPPy and PhPPh in dry and water saturated CD_2Cl_2 and $CDCl_3$ solvents were measured at $27 \pm 0.1°C$ on a Varian Inova four-channel 500 MHz Spectrometer. Some of these measurements were repeated to ensure the repeatability of the results, although due to shortage of model compounds we could not repeat all of them. The number of scans in these experiments varied from 100 to 100000 depending on the concentration of the samples. Generally, the number of scans increased as the concentration decreased.

For processing spectral data from ^{1}H NMR spectroscopy experiments, MestReNova software version 7.0.2 was used. For comparing spectra, the solvent peaks in each case were set as a reference peak. In the case of deuterated methylene chloride, CH_2Cl_2 was set to 5.32 ppm and in case of deuterated chloroform; $CHCl_3$ was set to 7.36 ppm. Also, for comparison of results in CDCl3 and CD_2Cl_2, the peak due to the internal reference, tetramethylsilane, was set as to zero.

For diffusion-ordered spectroscopy (DOSY) experiments, three concentrations of PyPPy in dry $CDCl_3$ solvent were prepared, 1×10^{-2} M, 5×10^{-4} M and 1×10^{-4} M. The DOSY experiments were carried out on a Varian Inova four-channel 600 MHz spectrometer at 25 ± 0.1 °C(Durand et al., 2008). The pulse sequence followed Friebolin (2005).

T$_1$ measurement experiments were carried out on two concentrations of PyPPy in dry CDCl$_3$ solvent, 1 mM and 10 mM. These measurements were done at 27 ± 0.1 °C on a Varian Inova four-channel 500 MHz Spectrometer (Desando et al., 2010).

For temperature dependent experiments, ^{1}H NMR spectra of PhPPh in dry and water-saturated CDCl$_3$ were collected in a Varian Inova four-channel 400 MHz NMR instrument at selected temperatures, from -60 °C to +40 °C with +20 °C intervals and also in +55 °C.

Transverse Rotating-frame Overhauser Enhancement Spectroscopy, 2D-TROESY, (Abragam, 1983; Friebolin, 2005) experiments were done on two sample of PyPPy in dry CDCl$_3$ and were carried out on a Varian Inova four-channel 600 MHz spectrometer at 27.7 ± 0.1 °C (Hwang and Shaka, 1992).

pH dependent experiments were carried out on same concentration of PyPPy in acidic, basic and water saturated CDCl$_3$. 1H NMR spectra of these samples were collected on a Varian Inova four-channel 500 MHz spectrometer at 27 ± 0.1 °C.

3.3. Matrix-Assisted Laser Desorption Ionization –

Mass Spectrometer (MALDI)

Matrix-assisted laser desorption ionization – mass spectrometry (MALDI – MS) was used for checking the purity of the model compounds (Jagtap and Ambre, 2005). This MALDI – MS device was an Applied Biosystems/MDS SCIEX 4800 Plus MALDI TOF/TOF Analyzer. Model compounds were mixed with α-Cyano-4-hydroxycinnamic (HCCA) as the matrix in solution of Tetrahydrofuran (THF) and water. Then 0.5 μL of Samples were put on a 384 Opti-TOF 123 mm x 81 mm stainless steel plate by Applied Biosystems, which was then magnetically affixed to a 1016492B TES plate holder. For the data acquisition of ions, the MS Reflector Positive setting was used, with the laser intensity set to 3300.

4. Results and discussions

In this chapter results of association behaviour of 2,6-bis[2-(pyren-1-yl)ethyl]pyridine (PyPPy - $C_{41}H_{29}N$) and 2,6-bis[2-(phenanthren-9-yl)ethyl]pyridine (PhPPh - $C_{37}H_{29}N$) as models for asphaltene molecules are summarized.

4.1. Association behaviour of 2,6-phenanthrene-pyridine (PhPPh)

In this section, association behavior of PhPPh in deuterated chloroform and deuterated methylene chloride was investigated using ^{1}H NMR spectroscopy. Also, effects of temperature and water on association of this compound were investigated.

The assignment of carbons for PhPPh is shown in Scheme 4.1. For the attached protons, the number of the corresponding carbon is used. For example, HC_4 designates the two aliphatic protons which are attached to the number 4 carbon.
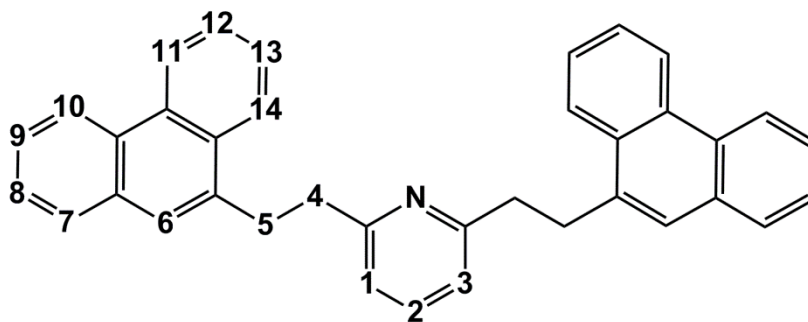
Scheme 4.1. Carbon assignment for PhPPh (symmetric structure)

4.1.1. ^{1}H NMR spectroscopy of 2,6-phenanthrene-pyridine (PhPPh) in dry $CDCl_3$

Six concentrations of PhPPh, from 1×10^{-2} to 10^{-5} M, were prepared in deuterated chloroform. After that, ^{1}H NMR spectra of these samples were collected in 500 MHz NMR instruments.

The ^{1}H NMR spectroscopy results of these samples suggested that the compound showed signs of aggregation in $CDCl_3$. Chemical shifts of different protons are summarized in table 4.1. For more comparisons, chemical shift of different protons in different concentrations are compared together (Figures 4.2 & 4.4). The spectra of different concentrations are stacked together to show the trend for each of the protons (Figures 4,1 & 4. 3).

	1×10^{-2} (M)	1×10^{-3} (M)	5×10^{-4} (M)	1×10^{-4} (M)	5×10^{-5} (M)	1×10^{-5} (M)
HC_4	3.35	3.34/3.82	3.35/3.84	3.84	3.383	3.84
HC_5	3.62	3.62/3.89	3.62/3.9	3.9	3.9	3.9
HC_1 & HC_3	6.97	6.97	6.96	6.91	6.91	6.91
HC_2	7.44	7.44	7.44	-	-	-
HC_7	7.79	7.79	7.78	-	-	-
HC_{14}	8.29	8.27	8.27/8.23	8.23	8.23	8.23
HC_{10}	8.68	8.67	8.66	8.65	8.65	8.65
HC_{11}	8.77	8.77	8.76	8.76	8.76	8.76

Table 4.1. ^{1}H NMR spectroscopy chemical shift of protons of PhPPh in dry $CDCl_3$ (in ppm)
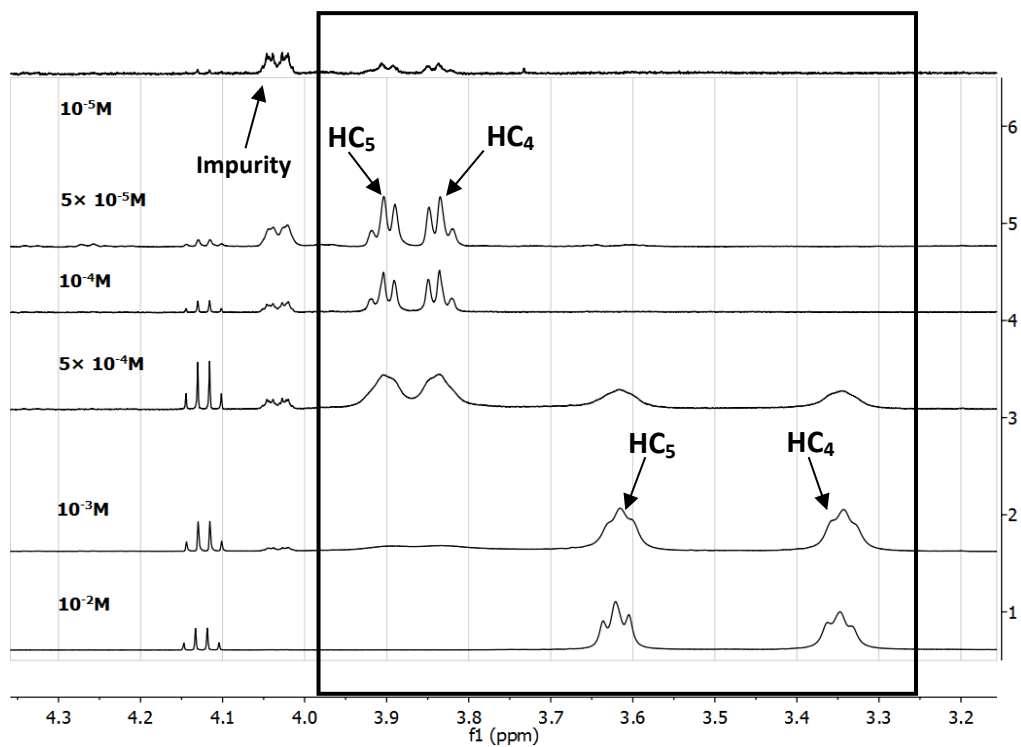
Figure 4.1. ^{1}H NMR spectroscopy results methylene (CH$_2$) groups of PhPPh in CDCl$_3$ over a range of concentrations
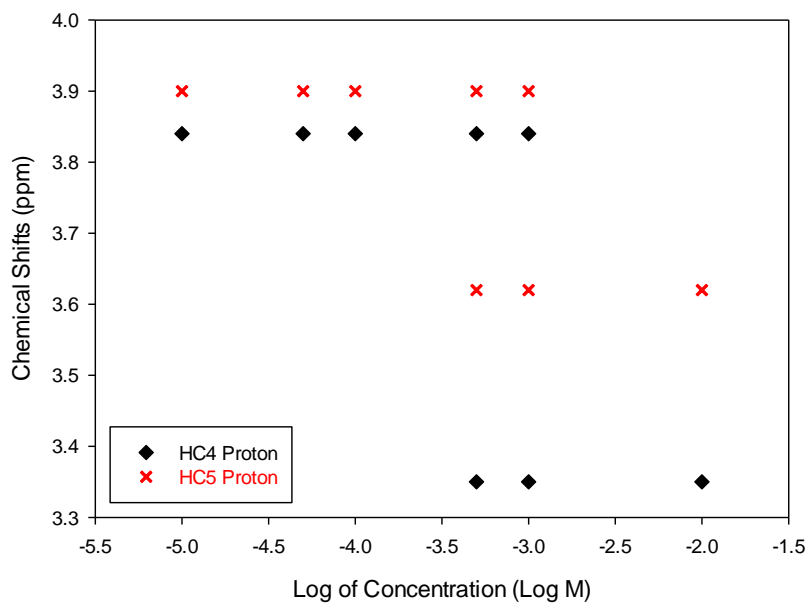
Figure 4.2. ^{1}H NMR spectroscopy chemical shift of HC$_4$ & HC$_5$ as a function of concentration

As shown in Figure 4.2, the chemical shift of HC_4 and HC_5 moved upfield (decreasing chemical shift) with increasing concentration from 1×10^{-5} M to 1×10^{-2} M. The behavior illustrated in Figure 4.2 is a jump in the chemical shift, likely due to a change in conformation, rather than a gradual shift. The results show a clear multiplicity of signals from the same protons in the chemical structure, suggesting the presence of more than one conformation. There is no change for chemical shift of protons when the concentration is between 1×10^{-4} M and 1×10^{-5} M. At intermediate concentrations of 1×10^{-3} M and 5×10^{-4} M, two interesting results are observed:

(1) The line widths of signals are significantly larger than at other measured concentrations as shown in Figure 4.2 and 4.3;

(2) Two different methlyene group signals are detected as shown in Figure 4.1.

Also, blank deuterated chloroform was investigated to confirm that the peaks at 4.03 and 4.12 ppm are related to impurities from solvent and compound, respectively. The impurity from the solvent can be related to a compound such as a plasticizer.
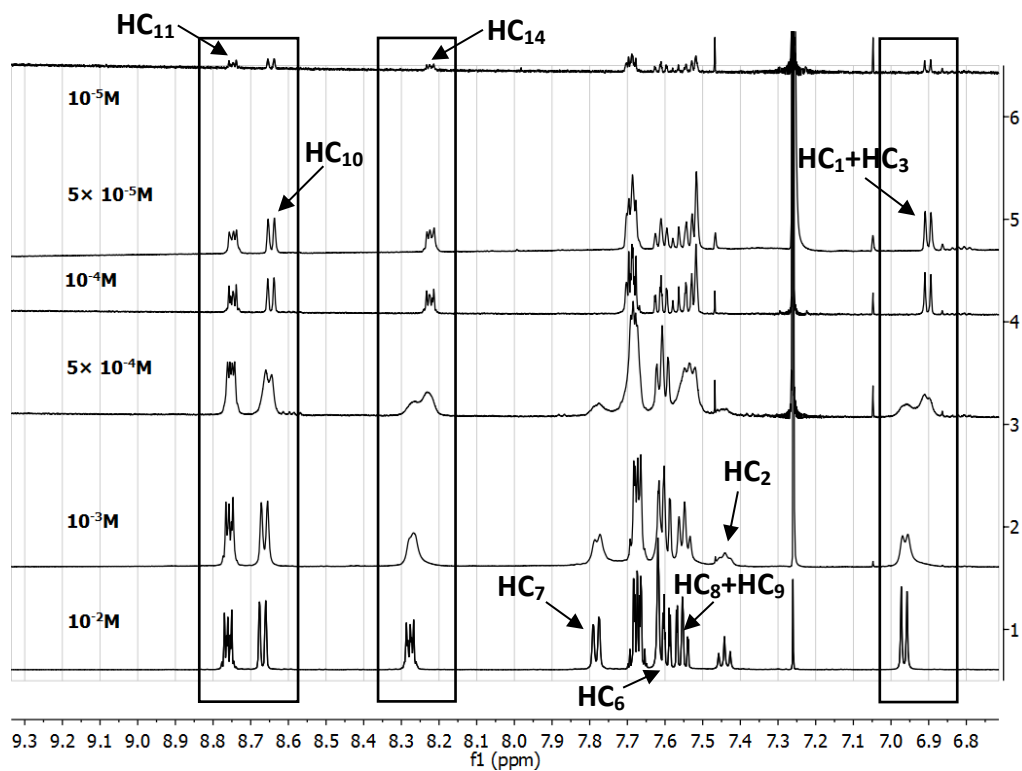
Figure 4.3. ^{1}H NMR spectroscopy results of aromatic protons of PhPPh in CDCl$_3$ over a range of concentration
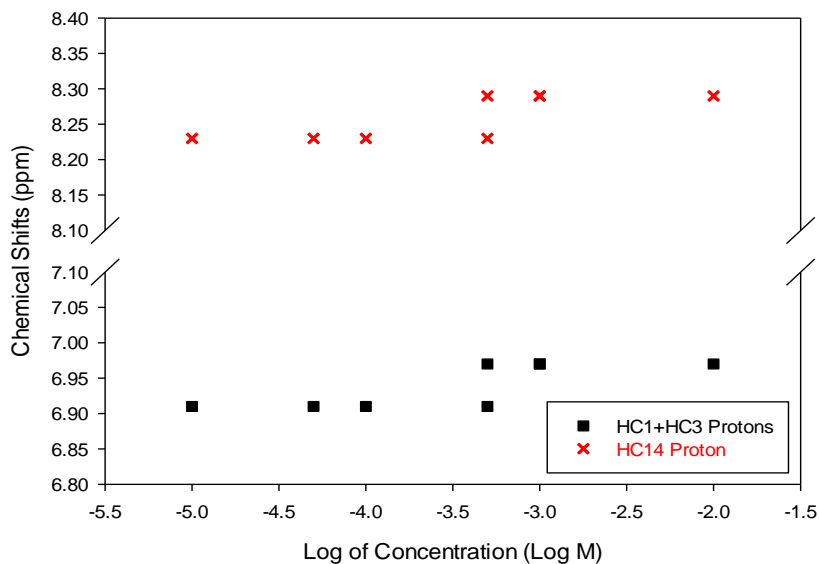
Figure 4.4. ^{1}H NMR chemical shift of HC$_{14}$ & HC$_1$+HC$_3$ as a function of concentration

Also, complex changes of ^1H NMR chemical shift for protons appeared in the aromatic regions of the spectra, for the protons on the phenanthrene and pyridine ring groups:

(1) The signals at 1×10^{-3} M and 5×10^{-4} M are broader than at other concentrations;

(2) The HC_1 and HC_3 from the pyridine ring moved upfield (increasing chemical shift of protons) with decreasing concentration. Two groups of signals are observed for HC_1 and HC_3 at 5×10^{-4} M;

(3) The signal of HC_2 from the pyridine ring first moved downfield with decreasing concentration and then likely overlapped with the signals of phenanthrene protons with further decrease in concentration , i.e. at 1×10^{-4} M or lower concentrations the signal of HC_2 is not distinct from other protons;

(4) The signal of HC_7 from phenanthrene protons first moves upfield with decreasing concentration and then overlaps with signals of other phenanthrene protons;

(5) The signals of HC_{14} move slightly upfield with decreasing concentration and at 5×10^{-4} M there are two groups of signals;

(6) The chemical shift of HC_6 from phenanthrene moved 0.1 ppm to upfield (increasing chemical shift from 7.52 ppm to 7.62 ppm) with decreasing concentration.

When the molecules aggregate in solution, we expect an increase in the local density of π electrons from the aromatic rings of nearby molecules. This change in electron density would then increase the chemical shift of protons,

moving them upfield (Shetty, Fischer, et al., 1996; Shetty, Zhang, et al., 1996; Fechtenkötter et al., 1999; Watson et al., 2004; Kastler et al., 2005). Increasing concentration would increase the shift by increasing the concentration of the aggregated species in proportion to non-aggregated species. However, the actual trend for protons HC_1, HC_3, HC_{14} and HC_6 is opposite to the expected one, because they shift downfield with increasing concentration, indicating a reduction in local electron density. This trend indicates that other interactions play an important role in the change of chemical shift of the protons.

The most important observation was the presence of two different groups of signals coexisting for HC_5, HC_4, HC_{14}, HC_1 and HC_3 at medium concentration, 5×10^{-4} M. We hypothesize that there are two different molecular conformations of PhPPh that give rise to these signals, due to two kinds of interactions in solution. As illustrated in Scheme 4.2, one type of interaction is intramolecular, where the molecules fold to bring π-electrons from one phenanthrene close to the middle pyridine ring and bridging carbons. This conformation of the molecule would be favored at low concentrations, where interactions between the molecules are not significant. At higher concentrations, intermolecular interactions appear and become dominant at the highest concentrations. Both types of interactions would be present in middle range of concentrations (See scheme 4.2). In other words, molecules of are folded monomer in dilute solutions and form dimers at high concentrations.
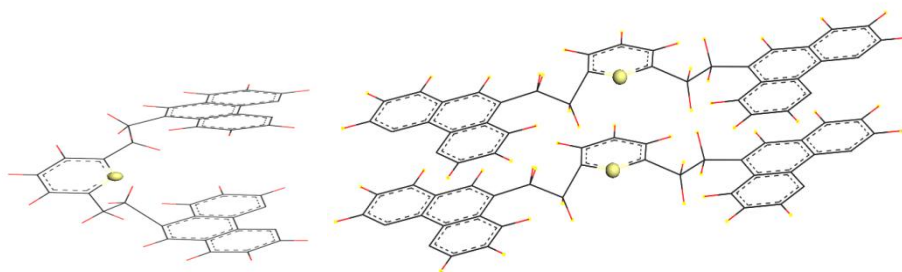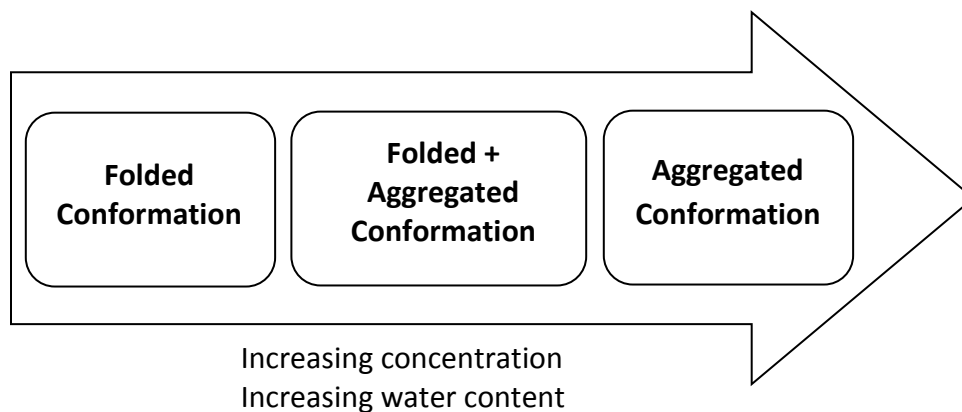
Scheme 4.2. Pathway of molecular conformation with changing concentration

According to the results of ^{1}H NMR spectroscopy, the main changes for chemical shifts belong to the aliphatic protons and pyridinc protons. Therefore, phenanthrene protons have a similar environment, or electron density, at both high and low concentrations, but the environment of pyridinc and aliphatic protons is different between low and high concentrations. According to the structure of folded and aggregated conformations (scheme 4.2), in both cases, phenantrene protons have the same environment with facing to another phenathrene ring, therefore they have same chemical shift which match with the experimental results. However, the electron density around aliphatic and pyridinic protons is different between two conformations which cause different chemical shifts. In

case of aggregated conformation (scheme 4.2), aliphatic protons have more shielding effect and therefore their chemical shifts move to upfield (Figure 4.1). Only some of phenanthrene protons, HC6 and HC14 which are near the aliphatic chain, have a small change in chemical shift (below 1ppm). These small changes can be related to changing the electron density of aliphatic chain. If someone considers that there is no aggregated conformation and there are only folded and unfolded conformations, therefore chemical shifts of phenanthrene protons have to move, but this effect was not observed.

The chemical shift in NMR spectroscopy represents the mean value from multiple time-averaged species (Martin, 1996), which indicates that the exchange between the monomers and aggregated molecules of 2,6- PhPPh in the solution is slow on the NMR time scale of circa 1 s. , The observation of separate signals for one proton in the monomers and aggregated molecules in the middle concentrations has been reported previously, and indicates exchange times longer than seconds. The broadening of the peaks of HC_4 and HC_5 at 5 x 10^{-4} M (Figure 4.1) suggests exchange rates in the range of milliseconds to one second (Luo and Mao, 1997; Gao and Wong, 1999; Sanna et al., 2006).

4.1.2. ^{1}H NMR spectroscopy of 2,6-phenanthrene-pyridine (PhPPh) in water saturated CDCl$_3$

Water can promote aggregation of organic compounds in solution via hydrogen bonding (Yan et al., 1999; Andersen et al., 2001; Zhang, Lopetinsky, et al., 2005; Zhang, Xu, et al., 2005; Zhang et al., 2007; Tan et al., 2009). To investigate the effect of water on self-association of PhPPh, two concentrations, 1×10^{-3} and 1×10^{-4} M, were prepared in water saturated CDCl$_3$ and ^{1}H NMR spectra of these samples were collected using a 500 MHz NMR instrument. The ^{1}H NMR spectra of these two samples are compared with the spectrum at the highest concentration tested in dry CDCl$_3$ (Figure 4.5 & 4.6).

The ^{1}H NMR spectroscopy results showed that the chemical shift for protons at 1×10^{-3} and 1×10^{-4} M in water saturated CDCl$_3$ is identical to the behavior at the highest concentration, 1×10^{-2} M, in dry CDCl$_3$. Therefore, the environment for each proton in water saturated CDCl$_3$ is the same with the environment at the highest concentration of solute in CDCl$_3$. Consequently, saturating the solvent with water had a similar effect to an increase in solute concentration, suggesting that water promoted the aggregation of the compound. Given the intermolecular and intramolecular interactions in solution, the intermolecular interaction of PhPPh is favourable in the presence of water even at very low concentration of solute. Organic molecules were shown to form stable complexes with water with forming O-H· · ·N hydrogen bonds and/or O-H· · ·π

interactions, as is the case of pyridine, 2,2′-bipyridine (Goldman, 1973; Bredas and Street, 1989; Goethals and Platteborze, 1992; Ruelle et al., 1992; Samanta et al., 1998; Tan et al., 2009). Therefore, we hypothesise that water molecules interact with the pyridyl nitrogen via forming hydrogen bonds, and then water molecules form hydrogen bonds with each other and help molecules to form the aggregated conformation. Modeling could be used to investigate the hypothesis that the intermolecular aggregate with hydrogen bonding to water provides the lowest energy state.
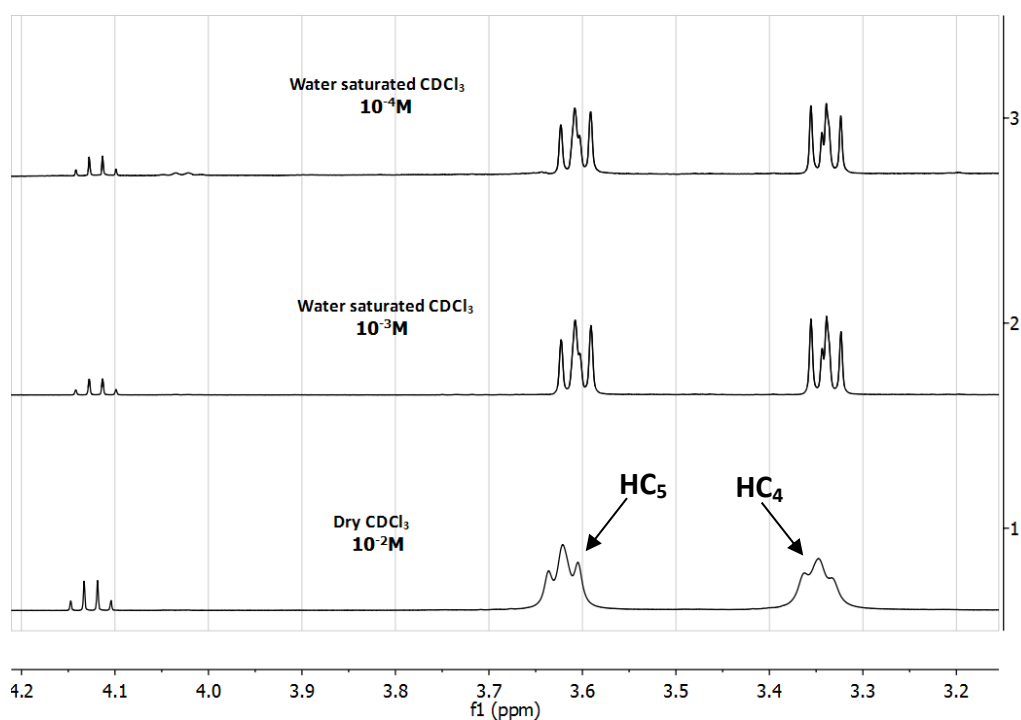
Figure 4.5. Comparison of ^{1}H NMR spectroscopy results 0.001 and 0.0001M in water saturated $CDCl_3$ and 0.01M in $CDCl_3$ (-CH2 group regions)
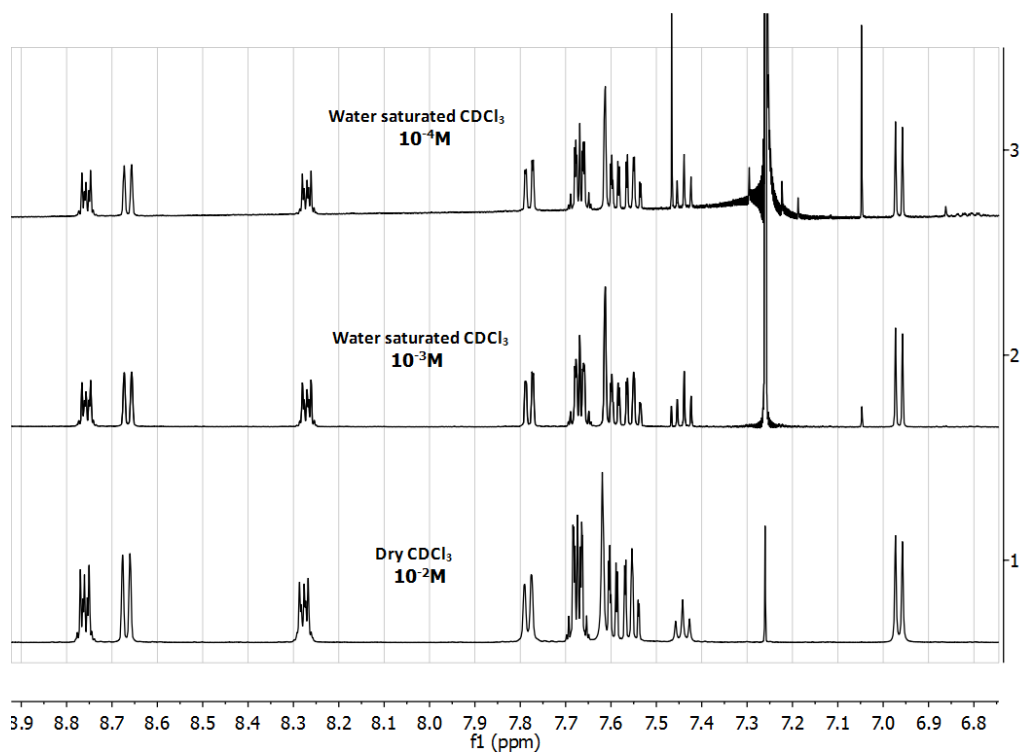
Figure 4.6. Comparison of ^{1}H NMR spectroscopy results 0.001 and 0.0001M in water saturated CDCl$_3$ and 0.01M in CDCl$_3$ (Aromatic region)

4.1.3. ^{1}H NMR spectroscopy of 2,6-phenanthrene-pyridine (PhPPh) in dry CD_2Cl_2

For investigating effects of solvent on self association, we changed the solvent from $CDCl_3$ to CD_2Cl_2.

Six different concentrations of PhPPh, from 2×10^{-2} M to 5×10^{-5} M, were prepared with dried CD_2Cl_2 then the ^{1}H NMR spectra of these samples were collected using a 500 MHz NMR instrument. The assignment of protons for 2,6-PhPPh is shown in Scheme 4.1. The chemical shift of protons are summarized in table 4.2 and ^{1}H NMR spectra of these samples are illustrated in Figures 4.7- 4.9.

Proton	Chemical Shift (ppm)
HC4	3.31 (Triplet peak)
HC_5	3.61 (Triplet peak)
HC_1 & HC_3	7.01 (Doublet peak)
HC_2	7.48 (Triplet peak)
HC_6	7.63 (Singlet peak)
HC_7	7.81 (Doublet peak)
HC_{10}	8.68 (Doublet peak)

Table 4.2. Chemical shift of protons of PhPPh in dry CD_2Cl_2
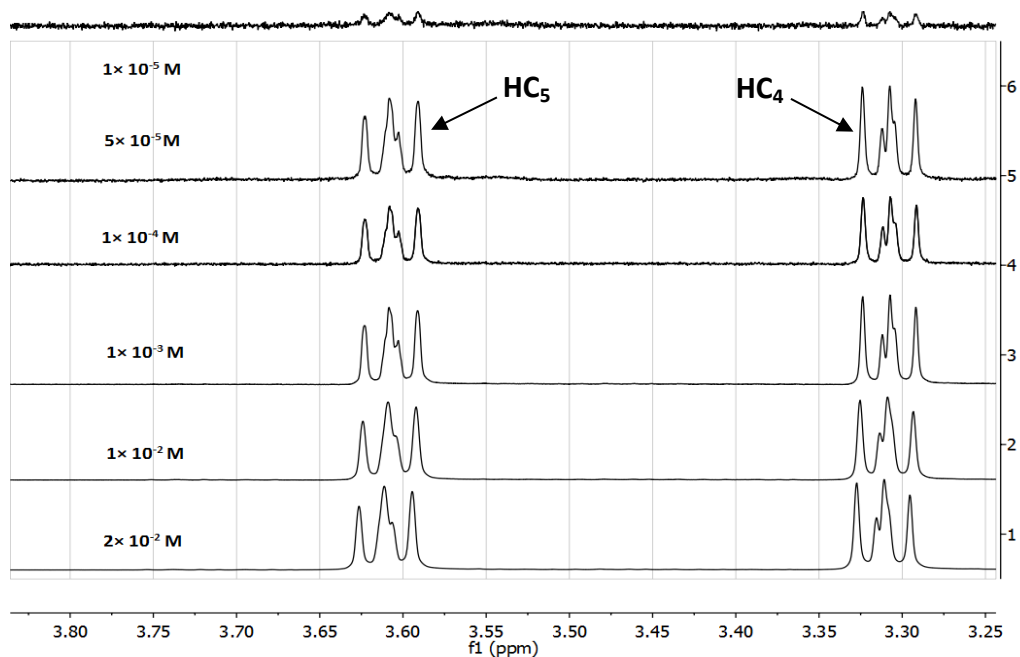
Figure 4.7. ^{1}H NMR spectroscopy results methyl groups of PhPPh in CD$_2$Cl$_2$ over a range of concentrations
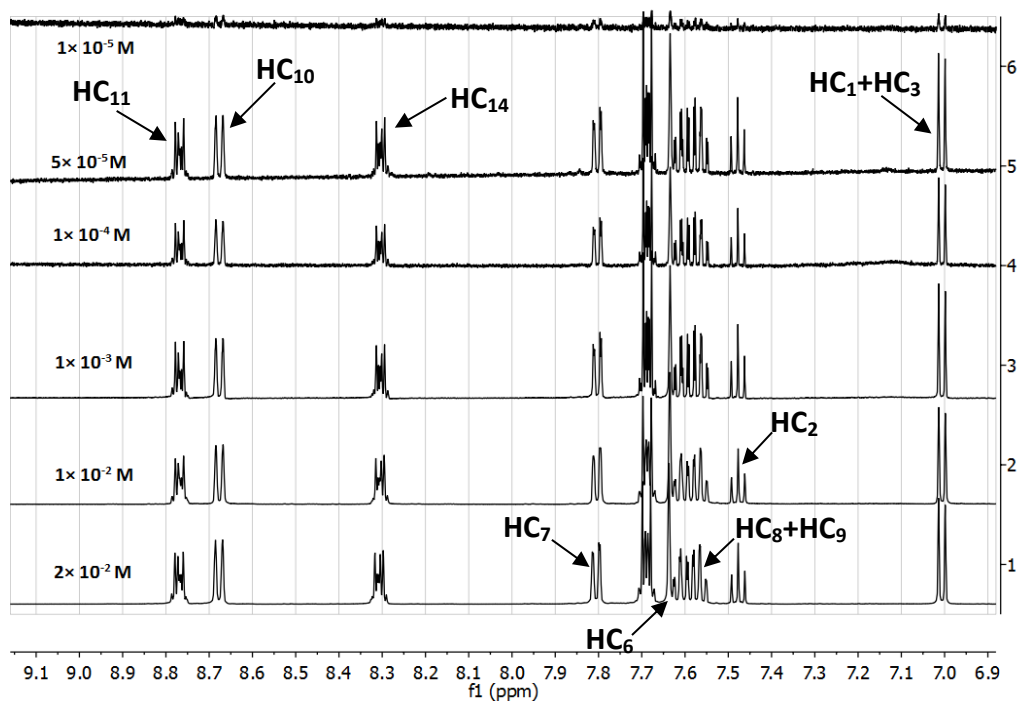
Figure 4.8. ^{1}H NMR spectroscopy results of aromatic protons of PhPPh in CD$_2$Cl$_2$ over a range of concentration

Interestingly, was no change of chemical shift for protons over this range of concentration. The chemical shifts for PhPPh in dry CD_2Cl_2 were the same as the results in water saturated CD_2Cl_2 and the highest concentration of solute in dry $CDCl_3$ (Figure 4.9). All protons of PhPPh have the same ^{1}H NMR chemical shift in all of these three environments; dry CD_2Cl_2, water saturated CD_2Cl_2, and dry $CDCl_3$.
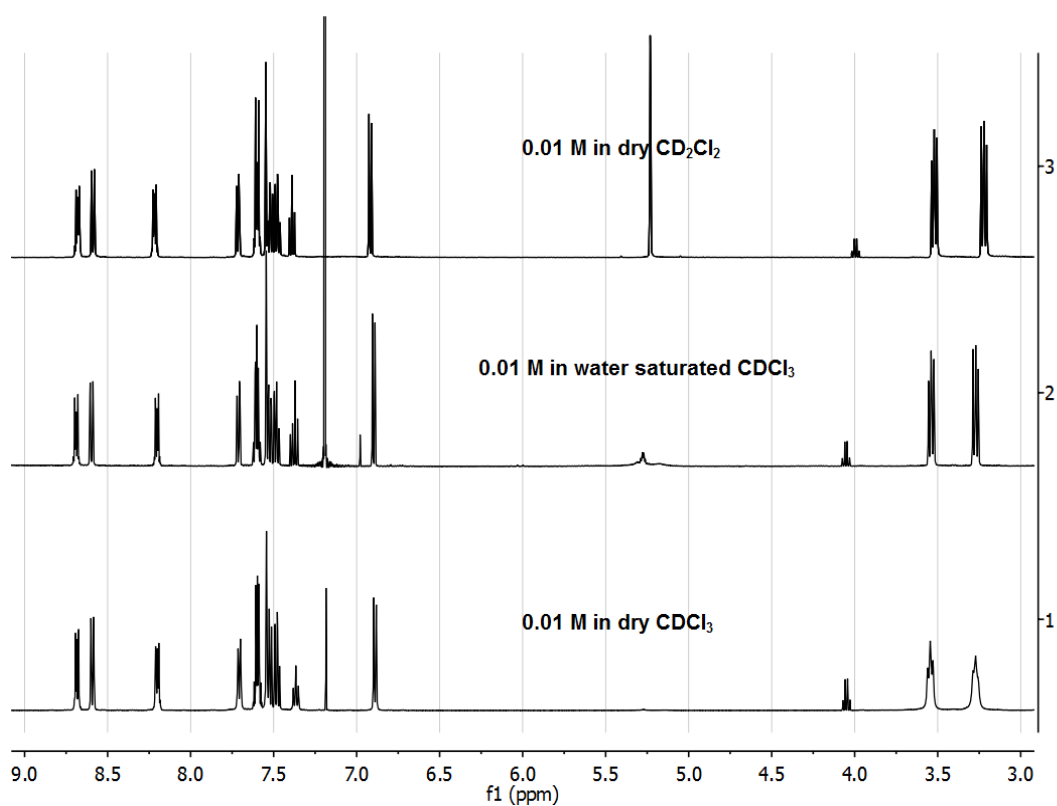
Figure 4.9. The comparison of the ^{1}H NMR spectroscopy results of PhPPh in dry CD_2Cl_2, $CDCl_3$ and water saturated $CDCl_3$

We conclude, therefore, that since PhPPh fully aggregates in the water saturated solvents and in the highest concentration in dry $CDCl_3$, it also fully

aggregates in this range of concentrations in dry CD_2Cl_2. More likely the CD_2Cl_2 interacts more weakly with the compound than $CDCl_3$, so there is less competition for unbinding between the PhPPh molecules.

4.1.4- ^{1}H NMR spectroscopy of 2,6-phenanthrene-pyridine (PhPPh) in Water saturated CD$_2$Cl$_2$

^{1}H NMR spectrum of PhPPh with concentration of 1×10^{-3} M in water saturated CD$_2$Cl$_2$ were collected in 500 MHz NMR instruments and compared with the results in the dry solvent (Figure 4.10). As discussed in section 3.1.2, the addition of hydrogen bonding would be expected to enhance complete aggregation in water saturated solvents. The lack of any impact of water on the chemical shifts in CD$_2$Cl$_2$ confirms that the compound is already fully aggregated.
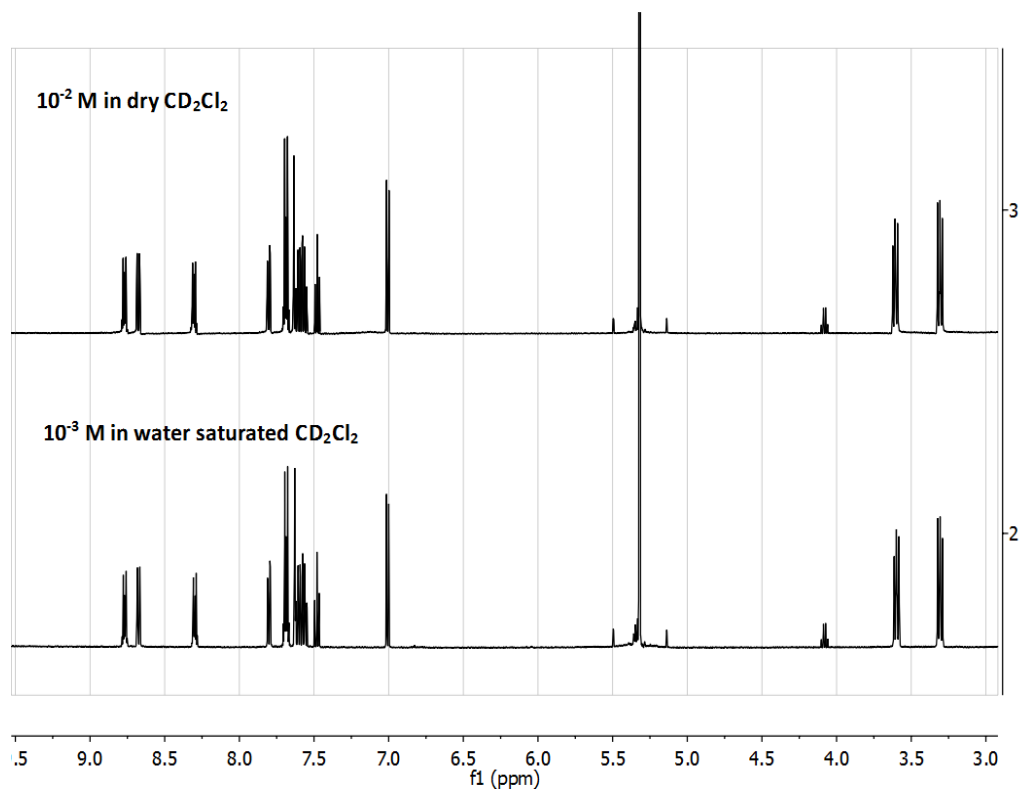
Figure 4.10. ^{1}H NMR spectroscopy results of PhPPh in water saturated and dry CD$_2$Cl$_2$

4.1.6. Temperature dependent studies of 2,6-phenanthrene-pyridine (PhPPh) in dry CDCl₃

Temperature may play role in association behaviour of PhPPh in organic solutions. High temperatures may cause aggregated conformation become less stable and convert to folded conformation

For investigating the effects of temperature on aggregation without the effect of water one concentration of PhPPh in CDCl₃ were prepared, 10^{-3} M. ^{1}H NMR spectra of these samples were collected in 400 MHz NMR instruments in selected temperatures, from -60°C to +40°C with +20°C intervals and also in +55°C.
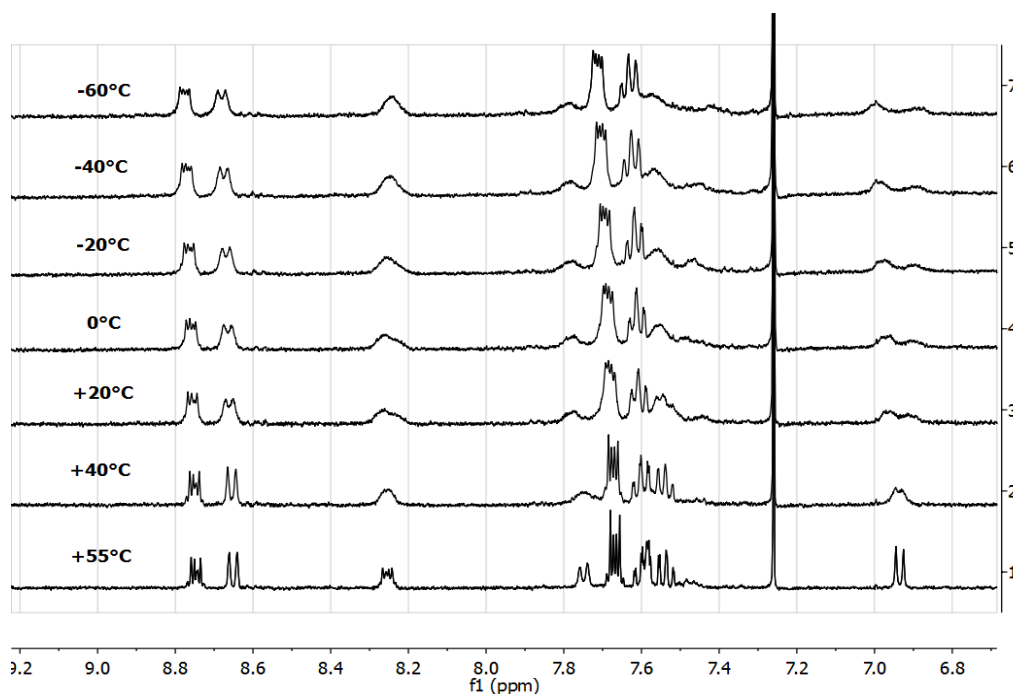
Figure 4.11. ^{1}H NMR spectroscopy results of temperature dependent studies of 0.001M of PhPPh in dry CDCl₃ (Aromatic regions)

HC_1+HC_3 protons move to downfield with decreasing temperature which means the aggregation behaviour caused by lowering temperature is same with increasing concentration. HC_7 proton moves to upfield with decreasing temperature, while and HC_{11}, HC_{10} and HC_{14} showed either no shift or minor shift as function of temperature. The results show that aggregation of PhPPh was temperature dependent and low temperatures are more favourable for aggregation. The thermodynamic properties of the interaction from temperature dependent experiments are calculated and summarized in table 4.3. For calculating equilibrium constant, K, a simple dimerization model was assumed:

$$2D \leftrightarrow D_2 \quad (1)$$

$$K = [D_2]/[D]^2 \quad (2)$$

The concentration of aggregated conformation (D_2) and folded conformation (D) were calculated by integration over signals of HC_1 and HC_3 protons which appeared in two regions at each temperature. It has been considered that in high temperature, which there is only on signal for HC_1 and HC_3, there is only folded conformation.

The van't Hoff equation was used to calculate ΔH and then ΔG.

$$\frac{d\ln K}{dT} = \frac{\Delta H}{RT^2} \quad (\text{Van}'\text{t Hoff equation}) \quad (3)$$

$$\ln\left(\frac{K_2}{K_1}\right) = -\frac{\Delta H}{R}\left(\frac{1}{T_2} - \frac{1}{T_1}\right) \quad (4)$$

$$\Delta G = -RT\ln K \quad (5)$$

	293.15 (K)	273.15 (K)	253.15 (K)	233.15 (K)	213.15 (K)
K (L mol^{-1})	3.58	3.28	3.01	2.6	2.6
ΔH (KJ mol^{-1})	-27.40±2	-27.40±2	-27.40±2	-27.40±2	-27.40±2
ΔG (KJ mol^{-1} K^{-1})	-19.94	-18.38	-16.86	-15.3	-14

Table 4.3. Thermodynamic properties of aggregation behaviour of PhPPh

Akbarzade et al. (Akbarzadeh et al., 2005) showed that for dipyrenyl dodecane dione, pyrenyl dodecanol and pyrenol the enthalpies of association are -77, -27 and -38 (kJ/mol), respectively. Therefore, our results of enthalpy of association of PhPPh are of the same order of magnitude with Akbarzadeh's work. Also, Kastler et al. (Kastler et al., 2005) show that for two hexabenzocoronenes with different length of attached alky chains, HBC-C14,10 and HBC-C12, enthalpies of association are -91.7 and -283(kJ/mol), respectively. These results for HBC are expected as they are larger molecules and have a higher enthalpy of association.

4.1.7. Temperature dependent studies of 2,6-phenanthrene-pyridine (PhPPh) in water saturated CDCl$_3$

Temperature may have some effect on formation of hydrogen bonds, which causes more aggregation (section 3.1.2), between PhPPh and water. Therefore, for investigating the effects of temperature on the aggregation, one concentration of PhPPh in water saturated deuterated chloroform was prepared, 10^{-3} M. After that, ^{1}H NMR spectra of this sample was collected in a 400 MHz NMR instrument in selected temperatures, from -60°C to +40°C with +20°C intervals and also in +55°C (Figure 4.12 & 4.13).
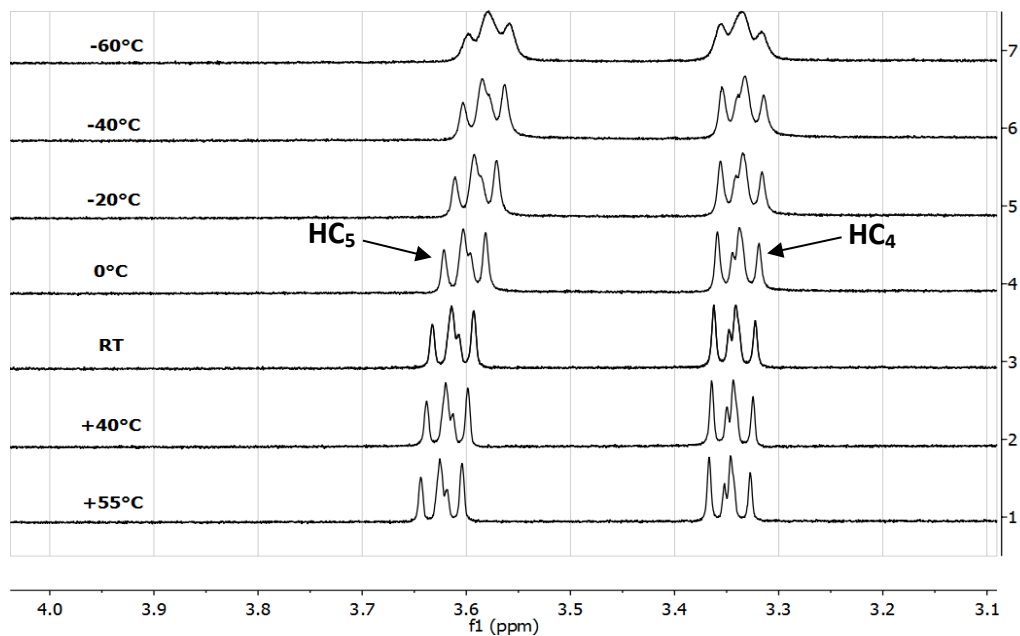
Figure 4.12. ^{1}H NMR spectroscopy results of temperature dependent studies of 0.001M of PhPPh in water saturated CDCl$_3$ (-CH2 group regions)
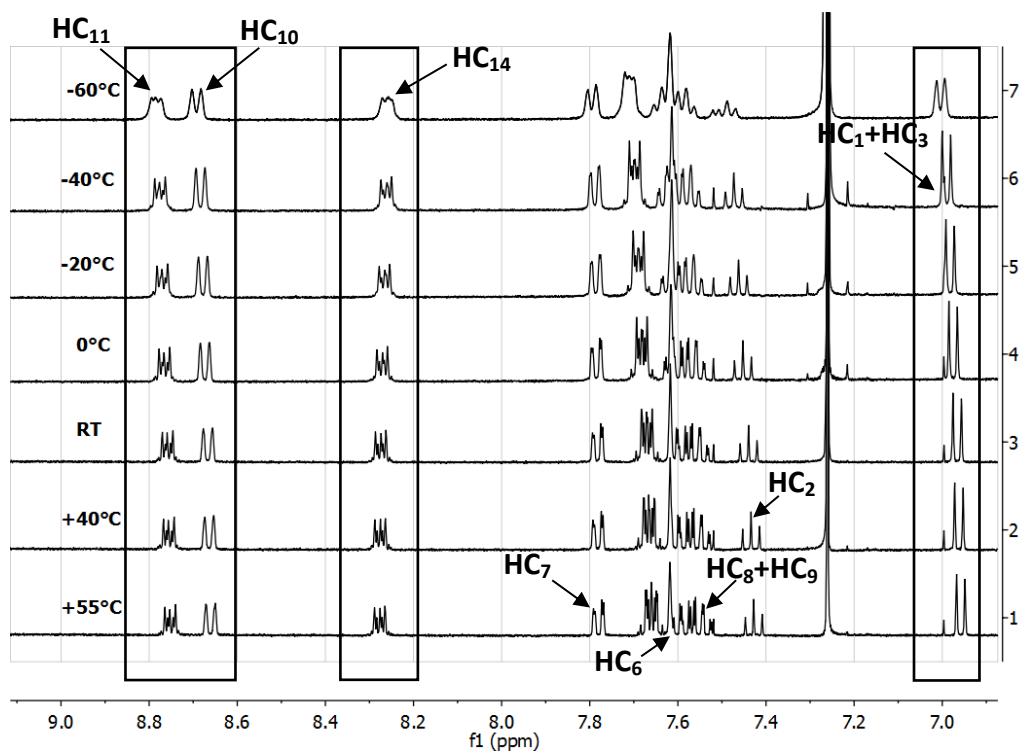
Figure 4.13. ^{1}H NMR spectroscopy results of temperature dependent studies of 0.001M of PhPPh in water saturated CDCl$_3$ (Aromatic regions)

All of the protons of PhPPh have a same chemical shift or minor change (less than 0.1 ppm) in this range of temperature in water saturated $CDCl_3$. The results showed that formation of hydrogen bond between water and PhPPh is not temperature dependent and aggregated conformation of PhPPh caused by water is stable in this range of temperature.

4.2 Association behavior of 2,6-pyrene-pyridine (PyPPy)

In section 3.1 association behavior of PyPPy was investigated and we hypothesize that there are two different conformations at low and high concentrations (Scheme 4.2). At low concentration, intramolecular interaction is favorable, while at high concentration intermolecular interaction is dominant. In this section, the consistency of this hypothesis was checked with investigation of association behavior of PyPPy in deuterated chloroform and deuterated methylene chloride using ^{1}H NMR titration, DOSY experiments, T_1 measurement and TROESY experiments. Also, effects of temperature, pH and water on association of this compound were investigated.

The assignment of carbons for 2,6- pyrene-pyridine is shown in Scheme 4.3. Each number is used for the corresponding to the protons which attached to that carbon.
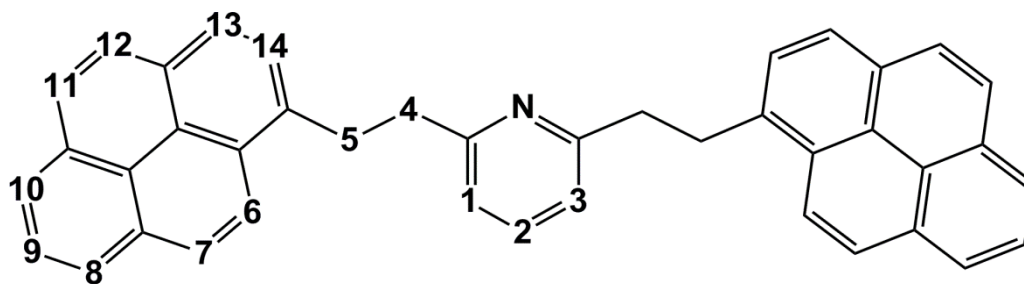
Scheme 4.3. Carbon assignment for PyPPy (symmetric structure)

4.2.1. ^{1}H NMR spectroscopy of 2,6-pyrene-pyridine (PyPPy) in dry CDCl$_3$

Six concentrations of this compound, from 1.5×10^{-2} to 5×10^{-5} M, were prepared in dry deuterated chloroform. After that, ^{1}H NMR spectra of these samples were collected in 500 MHz NMR instruments.

The ^{1}H NMR spectroscopy results of these samples suggested compound showed signs of aggregation in CDCl$_3$. Chemical shift of different protons are summarized in table 4.4 and the ^{1}H NMR spectra of the samples are stacked together for better comparison (Figure 4.14 and 4.16). Also, chemical shift of different protons in different concentrations were compared together (Figures 4.15 and 4.17).

	1.5×10^{-2}	1×10^{-2}	5×10^{-3}	1×10^{-3}	5×10^{-4}	1×10^{-4}	5×10^{-5}
HC_4	3.40	3.40	3.389	3.385/ 3.922	3.385/ 3.932	3.932	3.93
HC_5	3.861	3.863	3.856	3.851/ 4.061	3.848/ 4.069	4.075	4.075
HC_1 & HC_3	6.855	6.855	6.858	6.854/ 6.751	6.857/ 6.744	6.747	6.746
HC_2	7.342	7.345	7.347	7.358	7.395/ 7.353	7.403	7.403
HC_{14}	7.876	7.876	7.874	7.876	7.853	7.845	7.845
HC_{13}	8.397	8.397	8.396	8.387/ 8.375	8.360	8.352	8.351

Table 4.4. The chemical shift of protons of PyPPy in dry $CDCl_3$
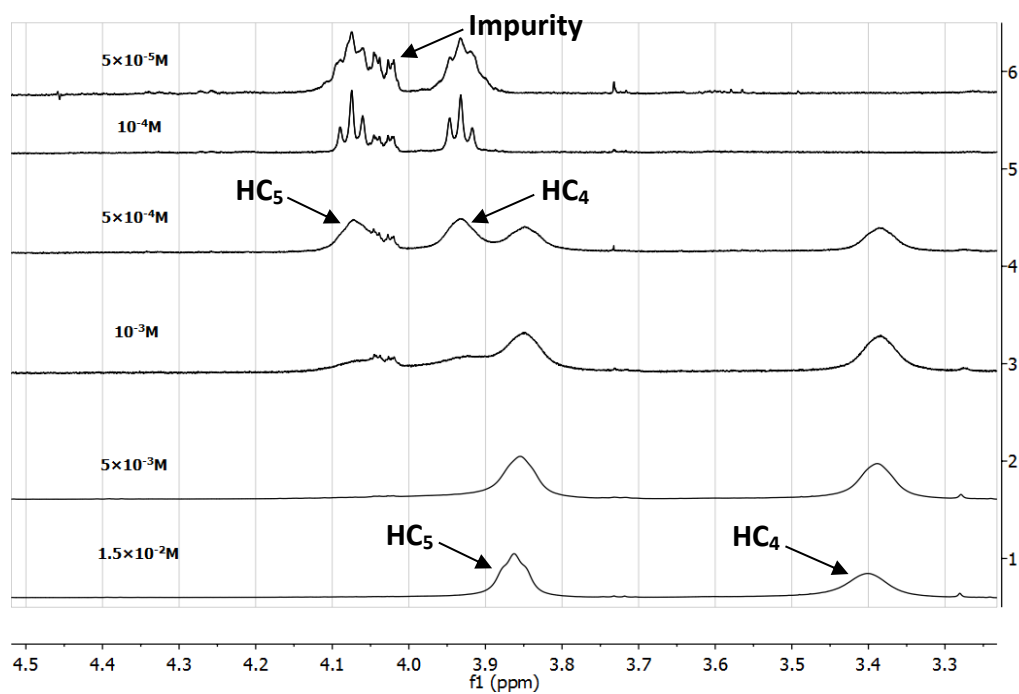
Figure 4.14. ^{1}H NMR spectroscopy results methyl groups of PyPPy in CDCl$_3$ over a range of concentrations
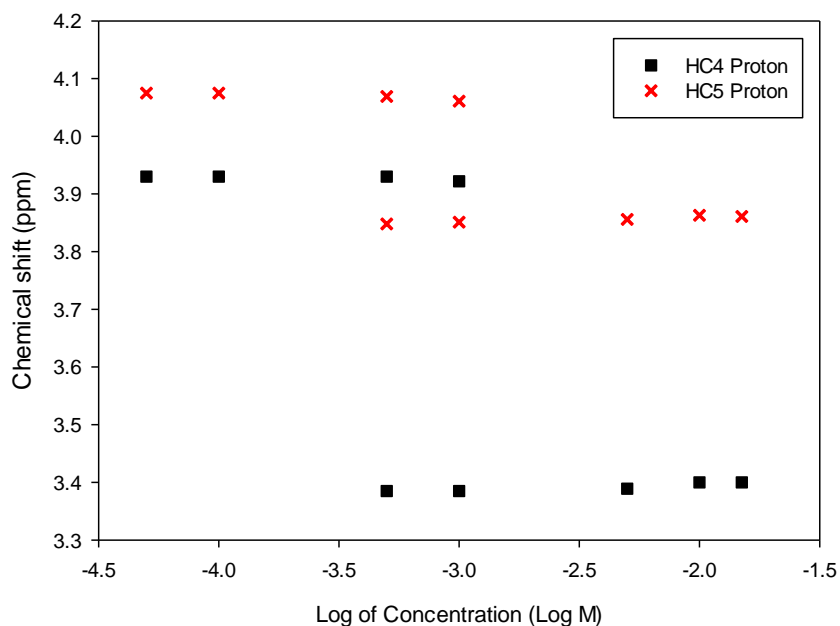
Figure 4.15. ^{1}H NMR spectroscopy chemical shift of HC$_4$ & HC$_5$ as a function of concentration

The chemical shift of HC$_4$ and HC$_5$ moved upfield (decreasing chemical shift) with increasing concentration from 5×10^{-4} M to 1.5×10^{-2} M (Figure 4.14 and 4.15). There is no change for chemical shift of protons when the concentration is lower than 1×10^{-4} M. At 1×10^{-3} M and 5×10^{-4} M, two different methylene group signals are present (Figure 4.14). The results show a clear multiplicity of signals from the same protons in the chemical structure, confirming the presence of more than one conformation.

Also, blank deuterated chloroform was investigated to confirm that the peaks at 4.03 and 4.12 ppm are related to impurities from solvent and compound, respectively. The impurity from the solvent can be related to a compound such as a plasticizer.
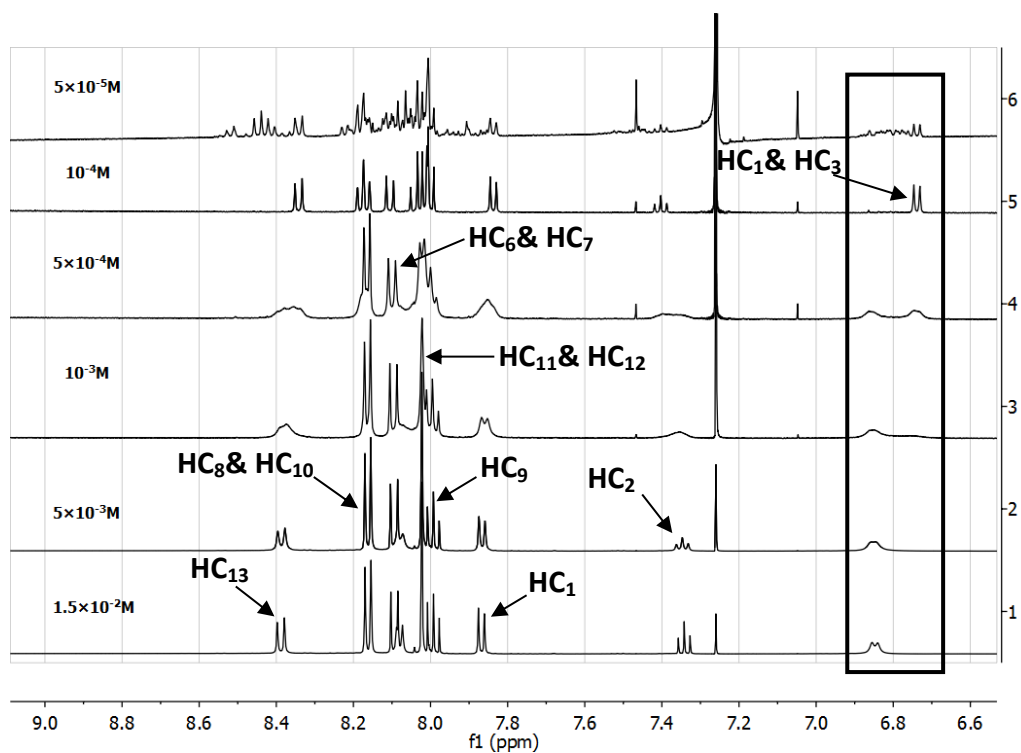
Figure 4.16. ^{1}H NMR spectroscopy results of aromatic protons of PyPPy in CDCl$_3$ over a range of concentration
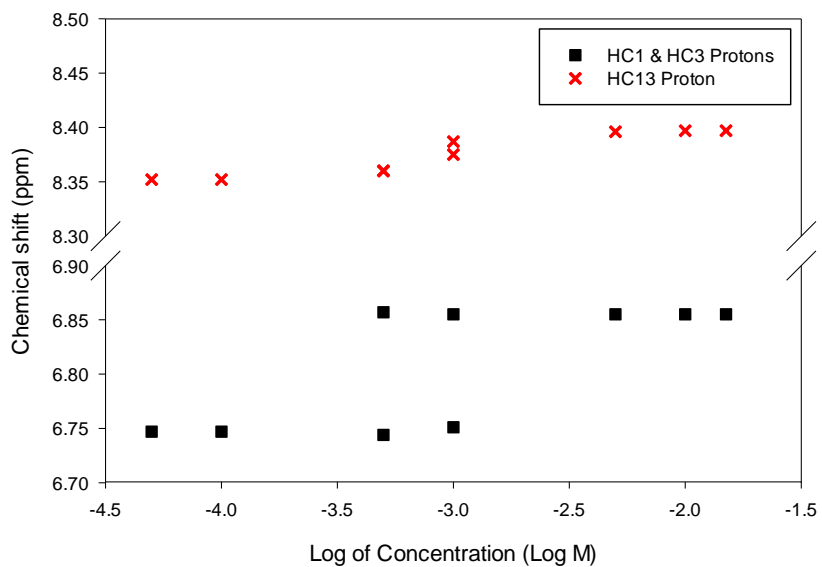
Figure 4.17. ^{1}H NMR chemical shift of HC$_{13}$, HC$_1$ and HC$_3$ as a function of concentration

Complex changes of chemical shift for aromatic protons on the pyrene and pyridine rings are observed as a function of concentration:

(1) The signals at 1×10^{-3} M and 5×10^{-4} M are broader than at other concentrations;

(2) The HC_1 and HC_3 from the pyridine ring moved upfield (increasing chemical shift of protons) with decreasing concentration and two groups of signals are observed for HC_1 and HC_3 at 5×10^{-4} M;

(3) The signal of HC_2 from pyridine ring moved downfield with decreasing concentration;

(4) The signal of HC_9 from pyrene protons first move downfield with decreasing concentration and then are incorporated into signals of HC_{11} and HC_{12} protons;

(5) The signals of HC_{14} slightly move upfield with decreasing concentration.

(6) The HC_{13} move downfield with increasing concentration and two groups of signals exist for HC_{13} at 5×10^{-4} M.

As mentioned in section 3.1, when the molecules aggregate in solution, we expect an increase in the local density of π electrons from the aromatic rings of nearby molecules. This change in electron density would then increase the chemical shift of protons, moving them upfield (Shetty, Fischer, et al., 1996; Shetty, Zhang, et al., 1996; Fechtenkötter et al., 1999; Watson et al., 2004; Kastler et al., 2005). Nonetheless, C_{14}, HC_1 and HC_3 protons moved to upfield with

decreasing concentration which is opposite of the expected one. These results are consistent with results of PhPPh, section 3.1.1. In addition, the presence of two groups of signals for HC_5, HC_4, HC_{13}, HC_2, HC_1 and HC_3 protons of PyPPy at middle concentrations is similar to the results of PhPPh (Section 3.1.1). Therefore, the aggregation mechanism for the two compounds is likely the same (Scheme 4.2).

4.2.2. ^{1}H NMR spectroscopy of 2,6-pyrene-pyridine (PyPPy) in water saturated CDCl$_3$

As mentioned in section 3.1.2, water can promote aggregation of organic compound in solutions via hydrogen bonding(Yan et al., 1999; Andersen et al., 2001; Zhang, Lopetinsky, et al., 2005; Zhang, Xu, et al., 2005; Zhang et al., 2007; Tan et al., 2009). For investigating effects of water on aggregation of PyPPy , one concentration, 1×10^{-3} M, were prepared in water saturated CDCl$_3$ and the ^{1}H NMR spectrum of the sample was collected in 500 MHz NMR instruments. The results were compared to results of 1.5×10^{-2} M in dry CDCl3 (Figure 4.18 and 4.19). Also, the chemical shift of protons was summarized in table 4.5.

	1×10^{-3}(water saturated CDCl$_3$)
HC$_4$	3.39
HC$_5$	3.848
HC$_1$ & HC$_3$	6.863
HC$_2$	7.345
HC$_{14}$	7.873
HC$_{13}$	8.395

Table 4.5. The chemical shift of protons of PyPPy in water saturated CDCl$_3$
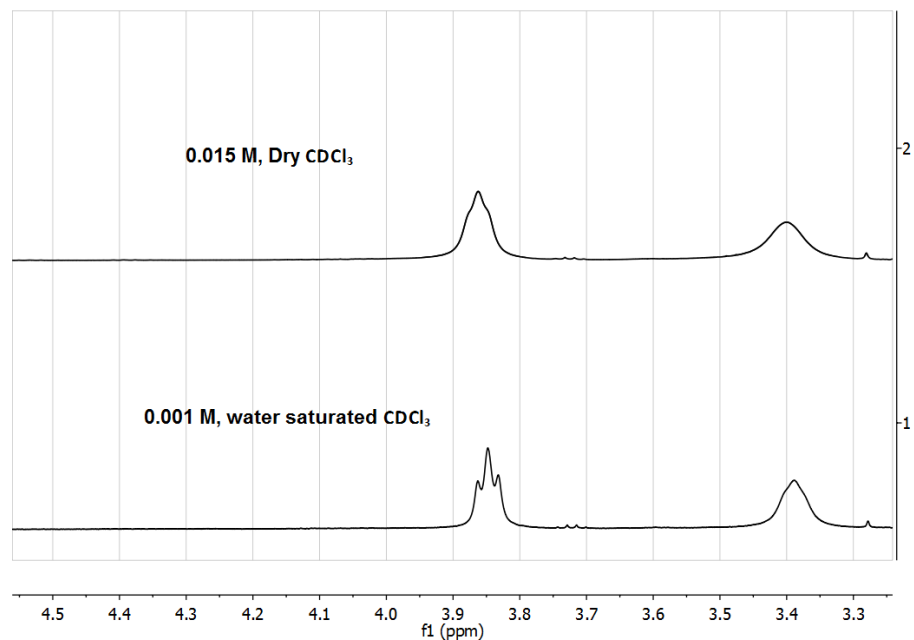
Figure 4.18. Comparison of ^{1}H NMR spectroscopy results 0.001M in water saturated CDCl$_3$ and 0.01M in CDCl$_3$ (-CH2 group regions)
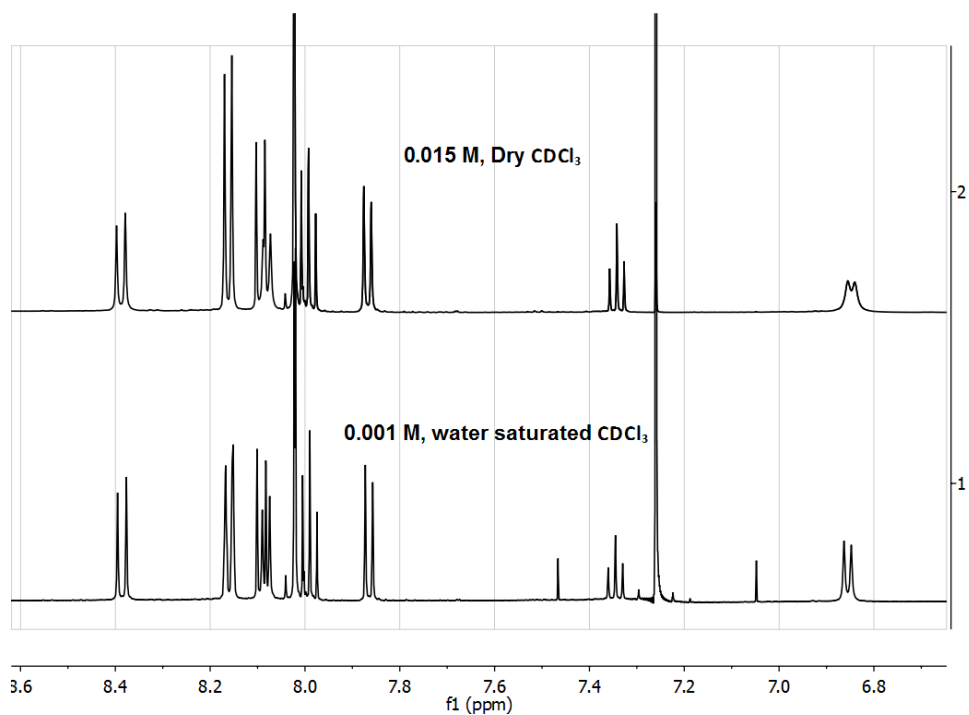
Figure 4.19. Comparison of ^{1}H NMR results 0.001M in water saturated CDCl$_3$ and 0.01M in CDCl$_3$ (Aromatic region)

Figure 4.18 and 4.19 show the ^{1}H NMR spectroscopy chemical shift for protons at 1×10^{-3} M in water saturated CDCl$_3$ is identical to those at 1.5×10^{-2} M in dry CDCl$_3$.. Therefore, the environment for each proton in water saturated CDCl$_3$ is the same with the environment at the highest concentration of solute in CDCl$_3$. As discussed for PhPPh in section 3.1.2, the intermolecular interaction of PyPPy is favourable in the presence of water even at very low concentration of solute. Organic molecules were shown to form stable complexes with water with forming O-H· · ·N hydrogen bonds and/or O-H···π interactions, as is the case of pyridine, 2,2′-bipyridine(Goldman, 1973; Bredas and Street, 1989; Goethals and Platteborze, 1992; Ruelle et al., 1992; Samanta et al., 1998; Tan et al., 2009). Therefore, this results confirmed the hypothesis that water molecules interact with the pyridyl nitrogen in folded monomers even in low concentrations and promote aggregation of molecules of solute via intermolecular interactions.

4.2.3. Effect of pH on aggregation of 2,6-pyrene-pyridine (PyPPy) in CDCl$_3$

Chloroform is naturally a little acidic and PyPPy is basic. For investigating whether acidity of the solvent has any effect on aggregation of model compounds of asphaltenes, the ^{1}H NMR spectra of 1×10^{-3} M of PyPPy in acid wash, water saturated and base wash CDCl$_3$ is compared(Figure 4.20 and 4.21).

	1×10^{-3}M (Water sat. CDCl$_3$)	1×10^{-3}M (Acidic CDCl$_3$)	1×10^{-3}M (Basic CDCl$_3$)
HC$_4$	3.390	3.400	3.400
HC$_5$	3.848	3.850	3.850
HC$_1$ & HC$_3$	6.863	6.860	6.864
HC$_2$	7.345	7.350	7.347
HC$_{14}$	7.873	7.870	7.873
HC$_{13}$	8.395	8.390	8.395

Table 4.6. The chemical shift of protons of PyPPy in acidic, water saturated and basic CDCl$_3$
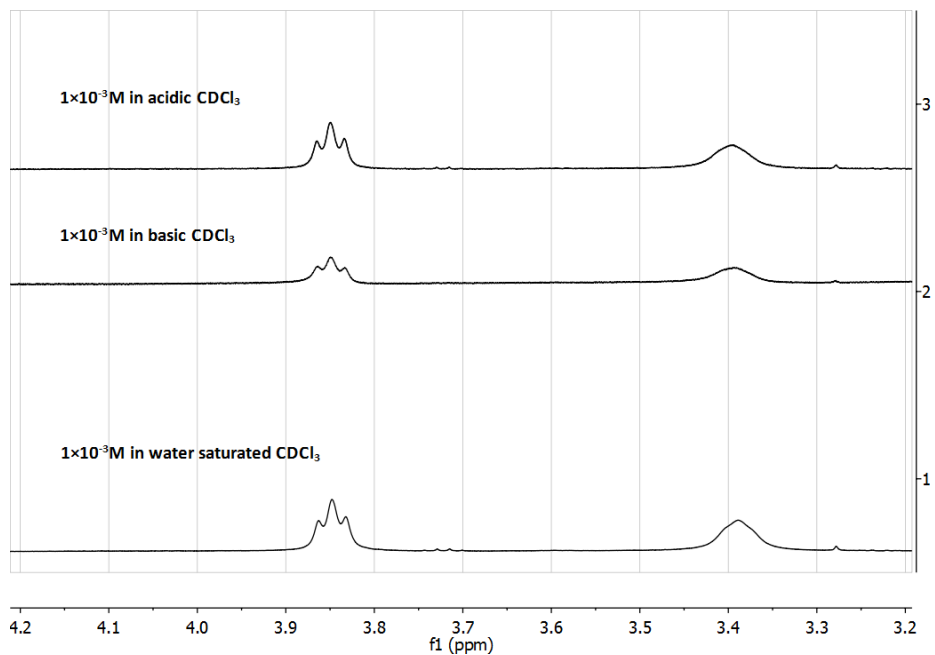
Figure 4.20. Comparison of ^{1}H NMR spectroscopy results 0.001M in acidic, water saturated and basic CDCl$_3$ (aliphatic region)
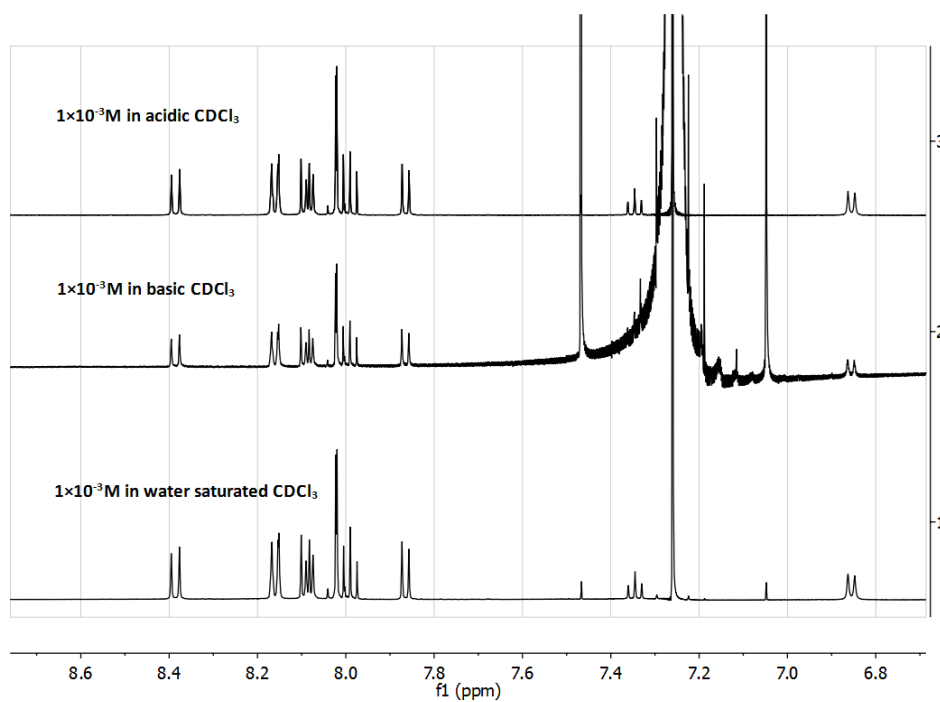
Figure 4.21. Comparison of ^{1}H NMR specroscopy results 0.001M in acidic, water saturated and basic CDCl$_3$ (aromatic region)

76

Figures 4.20 and 4.21 show that chemical shift of each protons of PyPPy is same in all acidic, water saturated and basic solution. Therefore, pH has no effect on aggregation of PyPPy in $CDCl_3$ and water can form hydrogen bonding with the solute independent of pH.

4.2.5. 2D-TROESY (Transverse Rotating-frame Overhauser Enhancement Spectroscopy) experiments on 2,6-pyrene-pyridine (PyPPy) in CDCl$_3$

This technique provides correlations based on through-space interactions of protons (Hwang and Shaka, 1992a, 1992b). This technique is usually used to provide structural information about the molecules and can provide information about the protons have interaction together(Abragam, 1983; Bross-Walch et al., 2005; Friebolin, 2005). Therefore, 2D-TROESY experiments were done for PyPPy to identify which protons have interactions with each other from two different molecules or between two parts in one molecule.

Two concentrations of PyPPy in dry CDCl$_3$ were selected for TROESY experiments; 1×10^{-3} and 1.5×10^{-2} M, and these experiments were done in 500 MHz instrument. Unfortunately, lower concentrations cannot be applied because of low resolutions of results in low concentrations. Results of the TREOSY experiments are summarized in table 4.7 and 4.8 and also in figures 4.22 and 4.23. Each spot in the spectra show which protons have interaction with each other and stronger interactions have denser spots (Hwang and Shaka, 1992a, 1992b; Chmurny et al., 1993).
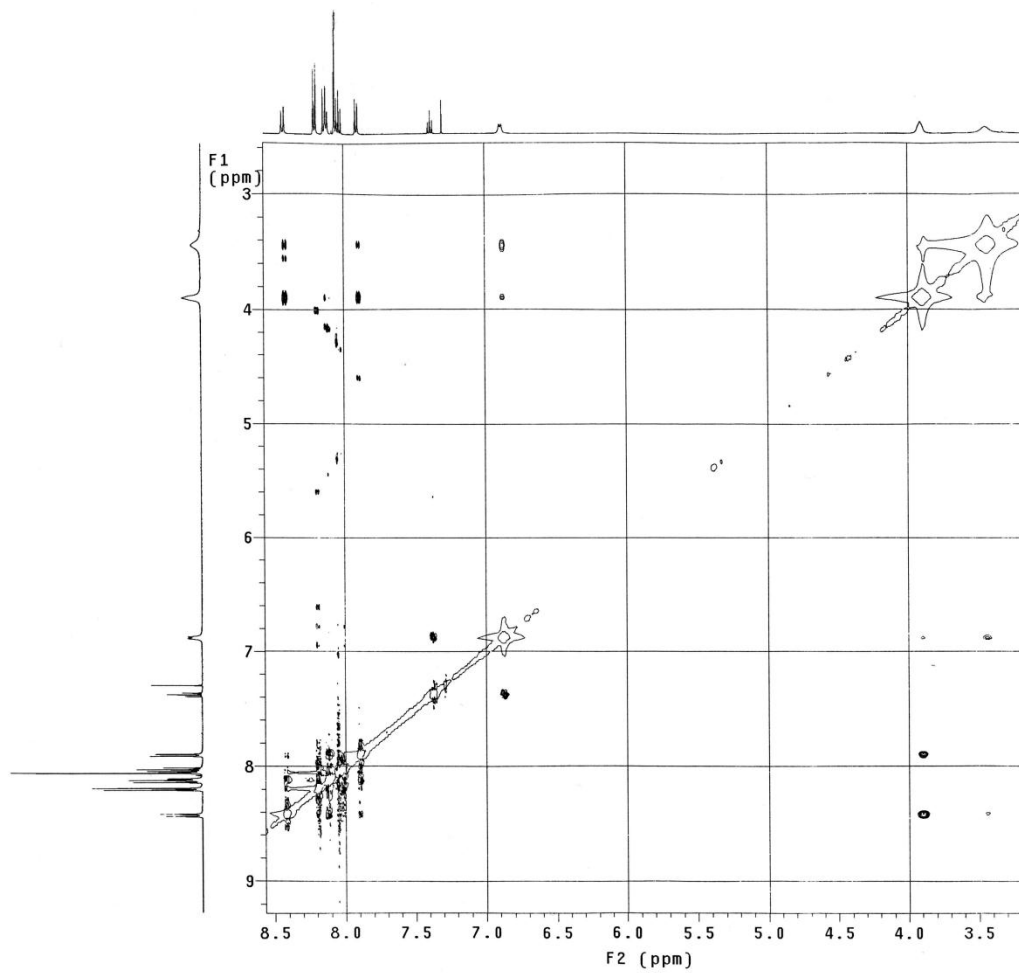
Figure 4.22. Results of TROESY experiments on 1.5×10^{-2} M of PyPPy in
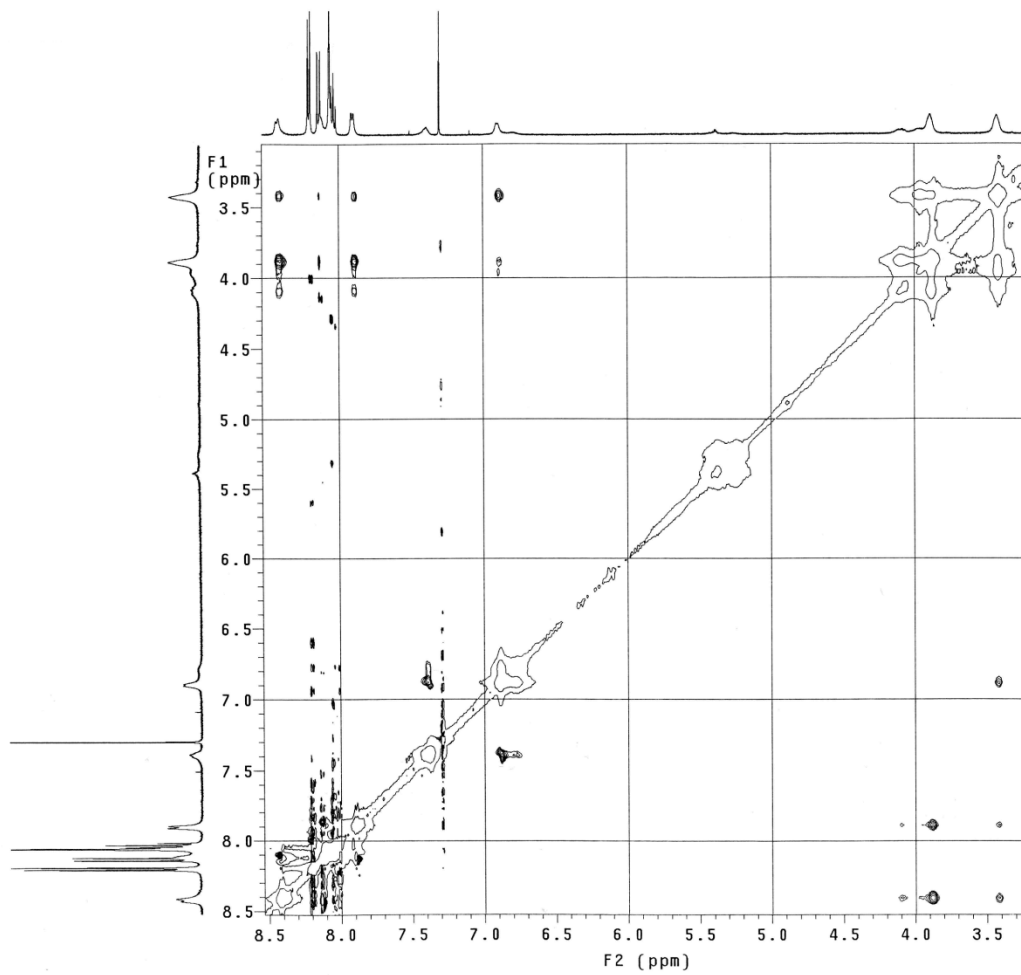
CDCl$_3$

Figure 4.23. Results of TROESY experiments on 1×10^{-3} M of PyPPy in CDCl$_3$

	HC$_4$	HC$_5$	HC$_1$ & HC$_3$	HC$_2$	HC$_{14}$	HC$_{13}$	HC$_9$	HC$_6$ & HC$_7$	HC$_8$ & HC$_{10}$
HC$_4$	+	-	+	-	+	+	-	-	-
HC$_5$	-	+	+	-	+	+	-	-	+
HC$_1$ & HC$_3$	+	+	+	+	-	-	-	-	-
HC$_2$	-	-	+	+	-	-	-	-	-
HC$_{14}$	+	+	-	-	+	-	-	+	-
HC$_{13}$	+	+	-	-	-	+	-	+	-
HC$_9$	-	-	-	-	-	-	+	-	+
HC$_6$ & HC$_7$	-	-	-	-	+	+	-	+	-
HC$_8$ & HC$_{10}$	-	-	-	-	-	-	+	-	+

Table 4.7. Results of interactions between different protons in solution of 1.5×10^{-2} M of PyPPy in CDCl$_3$. "+" shows there is interaction between protons and "-" means no interaction

	HC$_4$	HC$_5$	HC$_1$ & HC$_3$	HC$_2$	HC$_{14}$	HC$_{13}$	HC$_9$	HC$_6$ & HC$_7$	HC$_8$ & HC$_{10}$
HC$_4$	+	-	+	-	+	+	-	+	-
HC$_5$	-	+	+	-	+	+	-	+	-
HC$_1$ & HC$_3$	+	+	+	+	-	-	-	-	-
HC$_2$	-	-	+	+	-	-	-	-	+
HC$_{14}$	+	+	-	-	+	-	-	+	-
HC$_{13}$	+	+	-	-	-	+	-	+	-
HC$_9$	-	-	-	-	-	-	+	-	+
HC$_6$ & HC$_7$	+	+	-	-	+	+	-	+	-
HC$_8$ & HC$_{10}$	-	-	-	+	-	-	+	-	+

Table 4.8. Results of interactions between different protons in solution of 1 $\times$ 10^{-3} M of PyPPy in CDCl$_3$. "+" shows there is interaction between protons and "-" means no interaction

Unfortunately, due to low resolution of results because of low concentrations we cannot get much information from results of TROESY experiments. However, the results suggest that in 1×10^{-3} M, interaction between different protons in 1×10^{-3} M is different with interactions in 1.5×10^{-2} M. Some of interaction which only exist 1×10^{-3} M are only possible when a folded conformation (scheme 4.2) existed in the solution, i.e. interaction between HC$_6$-HC$_7$ and HC$_5$ and HC$_4$. Therefore, these results confirm the assignment of the signals at low concentration to a folded conformation that enabled these protons to interact.

4.2.6. T_1 (Spin-lattice or longitudinal relaxation time) measurement experiments

T_1 measurement is one of the methods which has been used to test this hypothesis that two different kinds of molecular structures and interactions exist at low and high concentrations. Despite the fact that the available experimental data for T_1 is always less than for chemical shift and coupling constant, several relationships between T_1 and molecular structures have been discovered and discussed(Friebolin, 2005). As it was discussed in literature background section, there are some parameters which affect T_1 such as molecular size, molecular shape, number of protons attached to nuclei and etc. (Abragam, 1983; Friebolin, 2005; Levitt, 2008). Generally, different molecules have different T_1 and in ^{1}H NMR, the relaxation time of ^{1}H is fairly short and in order of a few seconds the equilibrium will re-established, after a pulse is introduced to system to measure T_1 (Friebolin, 2005; Levitt, 2008). Also, it has been said that usually T_1 decreases when the mobility of molecules decreases (Friebolin, 2005). Therefore, if there are different structures of one compound in the solutions, different T_1 for the compound in those solutions may be obtained, because of the fact that different structure may have different mobility and average molecular size. As a result, T_1 measurement studies were done to test whether there are any differences between spine-lattice relaxation times of each proton in different concentrations.

Two concentrations of PyPPy in $CDCl_3$ were selected, 1 mM and 10 mM. Relaxation time measurement experiment on these samples were done in 500 MHz NMR instrument and results are summarized in table 4.9.

	T_1 for 1 mM (Second)	T_1 for 10 mM (Second)
HC_4	0.58	0.62
HC_5	0.56	0.65
HC_1 & HC_3	1.73	1.85
HC_2	1.63	1.83
HC_{14}	1.62	1.75
HC_9	2.00	1.10
HC_6 & HC_7	1.73	1.81
HC_8 & HC_{10}	1.96	2.07

Table 4.9. Results of T_1 measurements for 1 mM and 10 mM of PyPPy in $CDCl_3$ (Unit of T_1 is Sec.)

The unit of T_1 is in order of second. Therefore, the differences between measured T_1 for each proton for these two concentrations are significant (Desando et al., 2010). Two different measured T_1 for each proton in two different concentrations confirm existence of two different structures in solution.

Also, T_1 in higher concentration, 10 mM, is greater compared to lower concentration, 1 mM. These results suggest the less mobility of folded conformation (scheme 4.2) in deuterated chloroform because of its molecular structure which produces lower shielding effect compare to aggregated conformation.

4.2.7. Diffusion-Ordered Spectroscopy (DOSY) experiments

NMR diffusion experiment correlates chemical shift with molecular self diffusion coefficients of compounds in a mixture. It can be used to measure diffusion coefficients of different molecules according to shielding effects, caused by differences in the structure and composition of the molecule, as well as physical properties of the surrounding environment like temperature, viscosity and etc. (Abragam, 1983; Morris and Johnson, 1992; Friebolin, 2005; Levitt, 2008; Durand et al., 2009, 2010). Also, it is expected that DOSY provide valuable information concerning the physicochemical properties of molecules because it is sensitive to molecular weight and structure (Friebolin, 2005; Durand et al., 2010). In addition, self-diffusion coefficient of the solute depends strongly and nonlinearly upon all types of interactions; i.e. attractive solvent-solute interactions and attractive solute-solute interactions (Biswas et al., 1998). Therefore, if different structures of one compound have different shielding effect they will have different diffusion coefficients in a solvent, and NMR diffusion experiments can be used to test existence of these different structures in a solution. In this part of study, DOSY experiments were used to investigate whether there are any differences between diffusion coefficients of PyPPy in $CDCl_3$ with three different concentrations, 1×10^{-2} M, 5×10^{-4} M and 1×10^{-4} M.

For comparison of results of diffusion analysis on both the solvent or internal standard, TMS, were done in a single experiment and relative diffusivity

calculated (Table 4.10). Relative diffusivity is defined as the ratio of the diffusion coefficients of the solute and of the solvent or internal standard (Crutchfield and Harris, 2007; Durand et al., 2010).

$$D_{rel} = D_{solute}/D_{solvent} \qquad (6)$$

According to the Stokes-Einstein equation, this approach minimizes the impacts of viscosity or temperature variations between different measurements (Durand et al., 2010).

	Relative diffusivity based on TMS
1×10^{-2} M	0.40
5×10^{-4} M	0.38
1×10^{-4} M	0.35

Table 4.10. Results of diffusion coefficient of PyPPy in $CDCl_3$

Results show that diffusion coefficient is higher in high concentrations and it decreases with decreasing concentration. Different diffusion coefficients of solute means there are different structures and interactions in different concentrations. Also, molecules in high concentration have higher diffusivity and mobility which is consistent with the results of T_1 measurement experiments (section 3.2.6). Aggregated molecules have more shielding effect compare to folded conformation and can diffuse easier and have higher mobility in $CDCl_3$.

In addition, two groups of signals for HC_4 and HC_5 exist at 5×10^{-4} M which means two different diffusion coefficients for each of HC_4 and HC_5. This result also, confirms that we have two different structure and interaction in high and low concentration and in the middle concentration range both of the structures exist (Scheme 4.2).
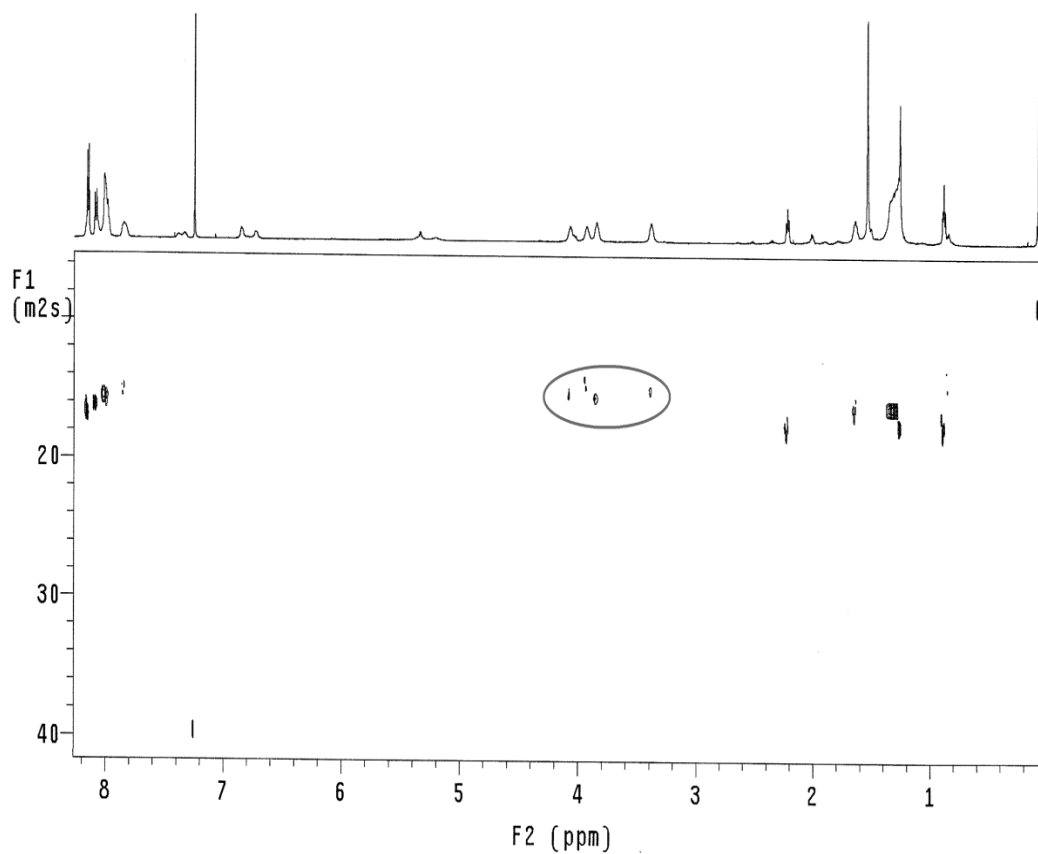
Figure 4.24. DOSY experiment on 5×10^{-4} M of PyPPy in $CDCl_3$

4.3. Comparison of results of ^{1}H NMR spectroscopy of 2,6-phenanthrene-pyridine (PhPPh) and 2,6-pyrene-pyridine (PyPPy)

For comparison of results of ^{1}H NMR spectroscopy of both compounds, the percent of aggregated conformation of each compound as function of concentration were calculated. For this approach, the ratios of integration over aliphatic protons in two regions of low and high concentration were calculated, with considering aggregated conformation in high concentration. PyPPy has larger π system and van der Waals surface area. However, the results show that at a same concentration, PhPPh has more tendency to form aggregated conformation (Figure 4.25). This result might be because of higher tendency of pyrene groups in PyPPy to form intramolecular interactions together via π-π stacking in folded conformation of this molecule. As a result, folded conformation of PyPPy could be more stable compared to the folded conformation of PhPPh. Therefore, PyPPy has higher onset of aggregation compared to PhPPh in these solvents.
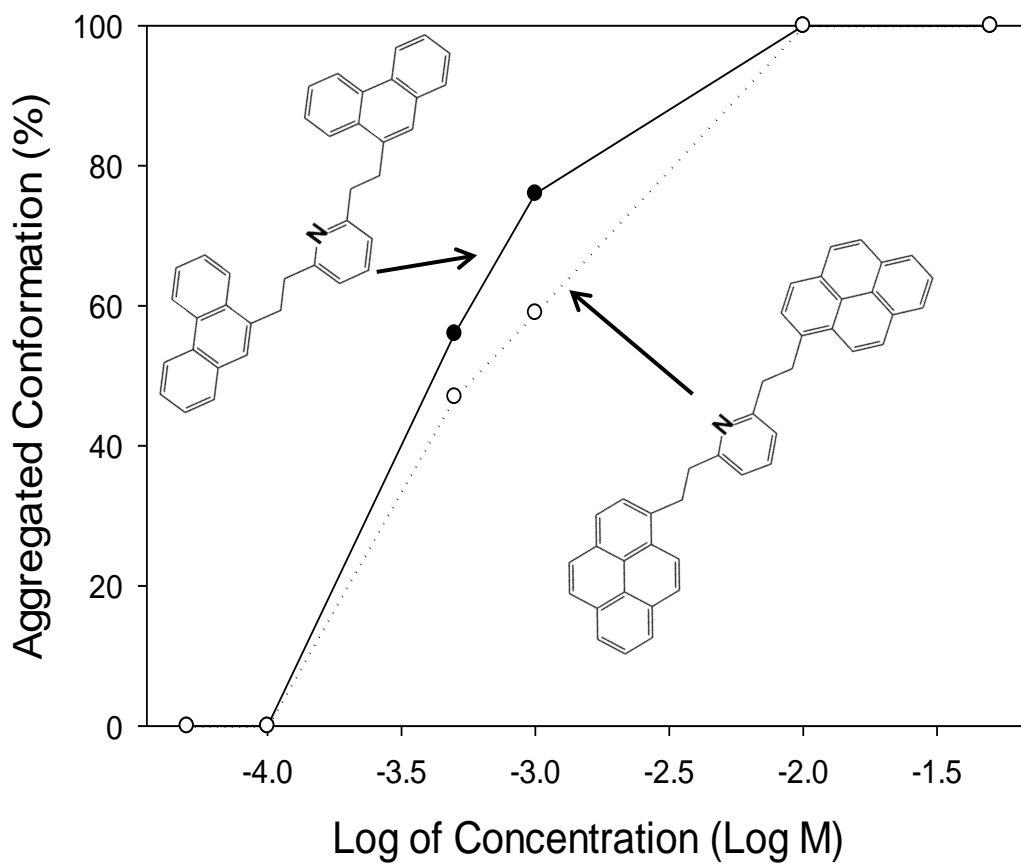
Figure 4.25. Percent of intermolecular conformation for PhPPh and PyPPy as a function of concentration

4.4. Summary and Implications

Both of 2,6-bis[2-(pyren-1-yl)ethyl]pyridine (PyPPy - $C_{41}H_{29}N$) and 2,6-bis[2-(phenanthren-9-yl)ethyl]pyridine (PhPPh - $C_{37}H_{29}N$) showed association behavior in deuterated chloroform and deuterated methylene chloride. These two compounds are models that mimic some chemical and physical behaviour of asphaltenes. The evidence for the existence of two conformations are:

1. Presence of two different groups of signals in coexisting for HC_5, HC_4, HC_1 and HC_3 at medium concentrations in ^1H NMR spectroscopy.

2. Different diffusion coefficient and spin-lattice relaxation time between low and high concentrations.

3. Coexistence of two groups of signals in diffusion ordered spectroscopy (DOSY) for aliphatic protons at medium concentrations.

These model compounds likely have folded conformation in dilute solutions and aggregated conformation in high concentrations (scheme 4.4). Intramolecular interactions to give a folded conformation are dominant in low concentrations; intermolecular interactions are dominant in high concentrations; and both conformations are present in the middle range of concentrations.

The evidence that these conformations are the most likely are:

90

1. Main changes in chemical shift in ^{1}H NMR spectroscopy are of aliphatic and pyridinic protons, which give shifts consistent with less shielding by nearby aromatic rings as the concentration is increased. A folded conformation at low concentration would give more shielding than a more planar stacked-aggregated conformation.

2. Small changes (below 1ppm) were observed in the chemical shifts of phenanthrene/pyrene protons in the ^{1}H NMR spectra as a function of concentration, which means they have same electron density at low and high concentrations. This result indicates that the large aromatic rings are always proximate to nearby aromatic rings, at all concentrations. In contrast, an unfolded, non-aggregated conformation would give shifts in the phenanthrene or pyrene protons relative to both the folded and the aggregated conformation. Although an open conformation would be expected to occur in equilibrium with the aggregated state, there was no evidence for a third conformation.

3. The results of DOSY and T_1 measurements are consistent with the existence of an aggregated conformation, which is more shielded compared to the folded conformation, at high concentrations. The same results confirmed the existence of a folded conformation at low concentrations which has low shielding effect and therefore low mobility.
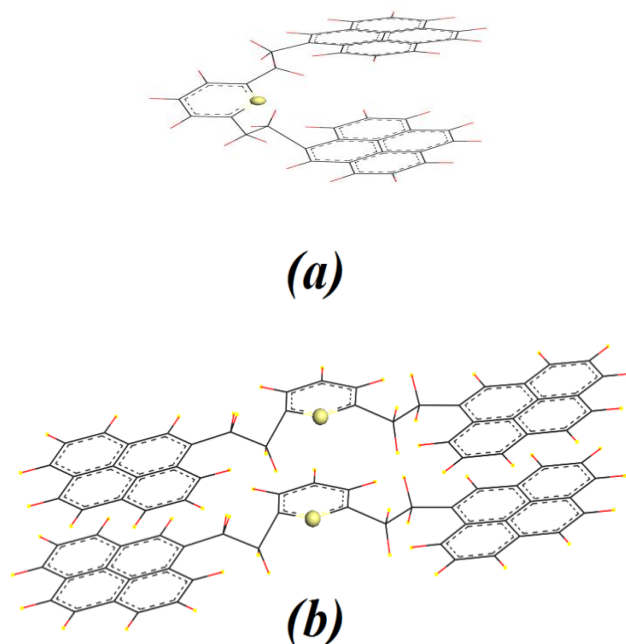
Scheme 4.4. (a) Folded conformation in low concentrations (intramolecular aggregation). (b) Aggregated conformation in high concentrations (intermolecular interaction)

Tan et al. (Tan et al., 2009) investigated self association of a pyrene derivative of bypyridine , 4,4′-bis(2-pyren-1-yl-ethyl)-2,2′-bipyridine (PBP). They reported changes in chemical shifts of protons of PBP consistent with increasing shielding with increasing concentrations, consistent with increased association behaviour for PBP. They observed increased shielding, i.e. upfield shifts, for all of the protons. The largest shifts were observed for the protons on the pyridine ring, rather than the methylene (CH$_2$) protons as observed in this study. The results of Tan et al. were consistent with open, unfolded conformation at low concentration and aggregated conformation at high concentration. In the case of PBP, folding conformations are not possible due to the length of the two pyridine rings bridged

between the pyrene rings, which increase the distance between pyrene groups in PBP compared to PyPPy. Therefore, pyrene groups in PBP cannot fold to face together and form a stable structure.

Trace amounts of water result in the aggregation of both compounds, even at low concentrations. Therefore, role of water to promote aggregation of asphaltenes via forming hydrogen bonding is confirmed. Moreover, lower temperatures are more favorable for aggregation of these compounds and pH has no effects on aggregation of this compound. The association properties of these two compounds confirmed that in addition to π-π interactions, other interactions play an important role in aggregation of asphaltenes such as hydrogen bonding with water. These results are consistent with recent work of Gray et al. (Gray et al., 2011).

The asphaltene fraction of an actual crude oil is much too complex a mixture to separate molecular species for direct investigation of the modes of intermolecular interactions in solution. Therefore, the observation of complex aggregation behaviour of model compounds is important to mechanisms of self-association of asphaltenes in solution. In the present study, aggregation was promoted by both the pyrene groups and hydrogen bonding of water to the pyridine rings, supporting the principle of supramolecular chemistry that multiple positive interactions promote aggregation. The same structures with benzene rings instead of pyridine did not exhibit aggregation in solution in chloroform (X Tan, personal communication, 2011). Given the significance of complex bridged structures in asphaltenes, the present study suggests that not only is intermolecular

association important in understanding asphaltene behavior, but also intramolecular interactions such as folding. The existence of a range of conformations may also be important in the slow rearrangement of asphaltenes on solid surfaces, observed in AFM studies, and at oil-water interfaces in water-in-oil emulsions to give rigid interfacial films.

The data from this study provides an excellent method to validate computational modeling methods. Modeling the ^{1}H NMR spectra of the two conformations and the concentration for transition between them provides a significant test of the ability to quantitatively model solution behavior. The role of water in the solvent phase provides an even more stringent test of association modeling. The possibility of different intra- and inter-molecular interactions even in simple models suggests that modeling the aggregation behavior requires consideration of a range of possible alternate conformations of the molecules. Clearly, modeling bridged flexible species is much more challenging than simple alkyl aromatics because of the dramatically increased number of interactions and degrees of freedom.

4.5. Recommendations for future studies

Interaction of different functional groups together can be studied by investigation of binary mixtures of model compounds using methods such as Fourier transform infrared spectroscopy (FTIR) in addition to ^{1}H NMR spectroscopy as in the present study. The addition of the acid-base interaction would be expected to give stronger interaction than observed on the present work. The pyridine-bearing compounds from this study can as act as the base compounds, and a carboxylic acid on a large aromatic group such as anthracene could provide the complementary structure. .

With the present pair of nitrogen compounds, water titration experiments can be done to determine the critical concentration of water for promoting aggregation.

Model compounds with longer alkyl bridge can be used to investigate effect of the length of the alkyl bridges between the aromatic ring l groups. Also, more bridge structures can be used to investigate their effects on aggregation, for example, more complex bridged structures may give internal folding as well as intermolecular aggregation.

References

1. Andersen, S., 1994. Effect Of Precipitation Temperature On The Composition Of N-Heptane Asphaltenes . Fuel Science & Technology International 12, 51-74.

2. Abragam, A., 1983. Principles of Nuclear Magnetism. Oxford University Press.

3. Agrawala, M., Yarranton, H.W., 2001. An Asphaltene Association Model Analogous to Linear Polymerization. Industrial & Engineering Chemistry Research 40, 4664-4672.

4. Akbarzadeh, K., Bressler, D.C., Wang, J., Gawrys, K.L., Gray, M.R., Kilpatrick, P.K., Yarranton, H.W., Carolina, N., Carolina, N., 2005. Association Behavior of Pyrene Compounds as Models for Asphaltenes. Energy & Fuels 8, 1268-1271.

5. Akbarzadeh, K., Dhillon, A., Svrcek, W.Y., Yarranton, H.W., 2004. Methodology for the Characterization and Modeling of Asphaltene Precipitation from Heavy Oils Diluted with n -Alkanes. Energy & Fuels 18, 1434-1441.

6. Alboudwarej, H., Beck, J., Svrcek, W., Yarranton, H., Akbarzadeh, K., 2002. Sensitivity of asphaltene properties to separation techniques . ENERGY & FUELS 16, 462-469.

7. Alshareef, A.H., Scherer, A., Tan, X., Azyat, K., Stryker, J.M., Tykwinski, R.R., Gray, M.R., 2011. Formation of Archipelago Structures during

Thermal Cracking Implicates a Chemical Mechanism for the Formation of Petroleum Asphaltenes. Energy & Fuels 25, 2130–2136.

8. Alshareef, A.H., Scherer, A., Tan, X., Azyat, K., Stryker, J.M., Tykwinski, R.R., Gray, M.R., 2012. Effect of Chemical Structure on the Cracking and Coking of Archipelago Model Compounds Representative of Asphaltenes. Energy & Fuels 26, 1828–1843.

9. Andersen, S.I., Manuel, J., Khvostitchenko, D., Shakir, S., Lira-galeana, C., 2001. Interaction and Solubilization of Water by Petroleum Asphaltenes in Organic Solution. Langmuir 17, 307-313.

10. Andreatta, G., Goncalves, C.C., Buffin, G., Bostrom, N., Quintella, C.M., Arteaga-Larios, F., Pérez, E., Mullins, O.C., 2005. Nanoaggregates and Structure−Function Relations in Asphaltenes. Energy & Fuels 19, 1282-1289.

11. Artok, L., Su, Y., Hirose, Y., Hosokawa, M., Murata, S., Nomura, M., 1999. Structure and reactivity of petroleum-derived asphaltene. Energy & Fuels 13, 287-296.

12. Asprino, O.J., Elliott, J. a. W., McCaffrey, W.C., Gray, M.R., 2005. Fluid Properties of Asphaltenes at 310−530 °C. Energy & Fuels 19, 2026-2033.

13. Auzély-Velty, R., Rinaudo, M., 2002. New Supramolecular Assemblies of a Cyclodextrin-Grafted Chitosan through Specific Complexation. Macromolecules 35, 7955-7962.

14. Biswas, R., Bhattacharyya, S., Bagchi, B., 1998. Molecular Theory for the Effects of Specific Solute-Solvent Interaction on the Diffusion of a Solute

Particle in a Molecular Liquid. The Journal of Physical Chemistry B 0, 3252–3256.

15. Boduszynski, M.M., 1987. Composition of heavy petroleums. 1. Molecular weight, hydrogen deficiency, and heteroatom concentration as a function of atmospheric equivalent boiling point up to 1400.degree.F (760.degree.C). Energy & Fuels 305, 2-11.

16. Bradley, E.K., Kerr, J.M., Richter, L.S., Figliozzi, G.M., Goff, D. a, Zuckermann, R.N., Spellmeyer, D.C., Blaney, J.M., 1997. NMR structural characterization of oligo-N-substituted glycine lead compounds from a combinatorial library. Molecular diversity 3, 1-15.

17. Bredas, J.L., Street, G.B., 1989. Theoretical studies of the complexes of benzene and pyrene with water and of benzene with formic acid, ammonia, and methane. JOURNAL OF CHEMICAL PHYSICS 7291–7299.

18. Bricout, H., Léonard, E., Len, C., Landy, D., Hapiot, F., Monflier, E., 2012. Impact of cyclodextrins on the behavior of amphiphilic ligands in aqueous organometallic catalysis. Beilstein Journal of Organic Chemistry 8, 1479-1484.

19. Bross-Walch, N., Kühn, T., Moskau, D., Zerbe, O., 2005. Strategies and tools for structure determination of natural products using modern methods of NMR spectroscopy. Chemistry & biodiversity 2, 147-77.

20. Buckley, J., 1996. Microscopic investigation of the onset of asphaltene precipitation. FUEL SCIENCE & TECHNOLOGY INTERNATIONAL 14, 55-74.

21. Buckley, J.S., 1999. Predicting the Onset of Asphaltene Precipitation from Refractive Index Measurements. Energy & Fuels 13, 328-332.

22. Buenrostro-Gonzalez, E., Lira-Galeana, C., Gil-Villegas, A., Wu, J., 2004. Asphaltene precipitation in crude oils: Theory and experiments. AIChE Journal 50, 2552-2570.

23. Cabrita, E.J., Berger, S., 2001. DOSY studies of hydrogen bond association: tetramethylsilane as a reference compound for diffusion studies. Magnetic Resonance in Chemistry 39, S142-S148.

24. Cardoza, L.A., Korir, A.K., Otto, W.H., Wurrey, C.J., Larive, C.K., 2004. Applications of NMR spectroscopy in environmental science. Progress in Nuclear Magnetic Resonance Spectroscopy 45, 209-238.

25. Chmurny, G.N., Paukstelis, J. V, Alvarado, A.B., Mcguire, M.T., Snader, K.M., Muschik, G.M., Hilton, B.D., 1993. NMR STRUCTURE Determination And Intramolecular Transesterification Of Four Diacetyl Taxinines Which Co-Elute With Taxol Obtained From Taxus X Media Hicksii Needles. Phytochemistry 34, 0–6.

26. Crutchfield, C. a, Harris, D.J., 2007. Molecular mass estimation by PFG NMR spectroscopy. Journal of magnetic resonance (San Diego, Calif. : 1997) 185, 179–82.

27. Desando, M. a, Lahajnar, G., Sepe, A., 2010. Proton magnetic relaxation and the aggregation of n-octylammonium n-octadecanoate surfactant in deuterochloroform solution. Journal of colloid and interface science 345, 338–45.

28. Dickie, J.P., Yen, T.F., 1967. Macrostructures of the asphaltic fractions by various instrumental methods. Analytical chemistry 39, 1847–1852.

29. Dickinson, E.M., 1980. Structural comparison of petroleum fractions using proton and 13C n.m.r. spectroscopy. Fuel 59, 290-294.

30. Durand, E., Clemancey, M., Lancelin, J.-M., Verstraete, J., Espinat, D., Quoineaud, A.-A., 2009a. Aggregation States of Asphaltenes: Evidence of Two Chemical Behaviors by 1 H Diffusion-Ordered Spectroscopy Nuclear Magnetic Resonance. The Journal of Physical Chemistry C 113, 16266-16276.

31. Durand, E., Clemancey, M., Lancelin, J.-M., Verstraete, J., Espinat, D., Quoineaud, A.-A., 2010. Effect of Chemical Composition on Asphaltenes Aggregation. Energy & Fuels 24, 1051-1062.

32. Durand, E., Clemancey, M., Lancelin, J.-M., Verstraete, J.J., Espinat, D., Quoineaud, A.-A., 2008. FUEL 4-H-1-DOSY NMR as a new method to analyze asphaltenes. ABSTRACTS OF PAPERS OF THE AMERICAN CHEMICAL SOCIETY, 236.

33. Durand, E., Clemancey, M., Lancelin, J.-M., Verstraete, J.J., Espinat, D., Quoineaud, A.-A., 2009b. Impact of chemical environment on asphaltenes

stability by 1H-DOSY NMR. ABSTRACTS OF PAPERS OF THE AMERICAN CHEMICAL SOCIETY, 238.

34. Durand, E., Clemancey, M., Quoineaud, A.-A., Verstraete, J., Espinat, D., Lancelin, J.-M., 2008. 1H Diffusion-Ordered Spectroscopy (DOSY) Nuclear Magnetic Resonance (NMR) as a Powerful Tool for the Analysis of Hydrocarbon Mixtures and Asphaltenes. Energy & Fuels 22, 2604-2610.

35. Espinat, D., Fenistein, D., Barré, L., Frot, D., Briolant, Y., 2004. Effects of Temperature and Pressure on Asphaltenes Agglomeration in Toluene. A Light, X-ray, and Neutron Scattering Investigation. Energy & Fuels 18, 1243-1249.

36. Eugen Scholz, 1984. Karl Fischer titration. Springer.

37. Fechtenkötter, A., Saalwächter, K., Harbison, M.A., Müllen, K., Spiess, H.W., 1999. Highly Ordered Columnar Structures from Heteronuclear Multiple-Quantum NMR Investigations. ANGEWANDTE CHEMIE-INTERNATIONAL EDITION 38, 3039–3042.

38. Fossen, M., Kallevik, H., Knudsen, K.D., Sj, J., 2011. Asphaltenes Precipitated by a Two-Step Precipitation Procedure . 2 . Physical and Chemical Characteristics. Energy & Fuels 25, 3552-3567.

39. Freund, H., Walters, C.C., Kelemen, S.R., Siskin, M., Gorbaty, M.L., Curry, D.J., Bence, a. E., 2007. Predicting oil and gas compositional yields via chemical structure–chemical yield modeling (CS-CYM): Part 1 – Concepts and implementation. Organic Geochemistry 38, 288-305.

40. Friebolin, H., 2005. Basic one- and two-dimensional NMR spectroscopy. Wiley-VCH.

41. Gao, X., Wong, T.C., 1999. Comment on "' Observation of exchange of small molecules between phases in a SDS micellar system '" Chemical Physics Letters 307, 62–66.

42. Gawrys, K.L., Blankenship, G.A., Kilpatrick, P.K., Carolina, N., 2006. On the Distribution of Chemical Properties and Aggregation of Solubility Fractions in Asphaltenes. Energy & Fuels 705-714.

43. Gawrys, K.L., Spiecker, P.M., Kilpatrick, P.K., 2003. The Role of Asphaltene Solubility and Chemistry on Asphaltene Aggregation. Petroleum Science and Technology 21, 461-489.

44. Goethals, M.., Platteborze, K., 1992. Infrared study of hydrogen bonds involving 2,2′-bipyridine and 2,2′-bipyrimidine. Influence of equivalent nitrogen atoms on the hydrogen bond strength. Spectrochimica Acta Part A: Molecular Spectroscopy 48, 671–681.

45. Goldman, S., 1973. The Determination and Statistical Mechanical Interpretation of the Solubility of Water in Benzene, Carbon Tetrachloride, and Cyclohexane. Canadian Journal of Chemistry 52, 1668–1680.

46. Gray, M.R., 2003. Consistency of Asphaltene Chemical Structures with Pyrolysis and Coking Behavior. Energy & Fuels 17, 1566-1569.

47. Gray, M.R., Tykwinski, R.R., Stryker, J.M., Tan, X., 2011. Supramolecular Assembly Model for Aggregation of Petroleum Asphaltenes. Energy & Fuels 25, 3125-3134.

48. Groenzin, H., Mullins, O.C., 1999. Asphaltene Molecular Size and Structure. The Journal of Physical Chemistry A 103, 11237-11245.

49. Groenzin, H., Mullins, O.C., 2000. Molecular Size and Structure of Asphaltenes from Various Sources. Energy & Fuels 677-684.

50. Groenzin, H., Mullins, O.C., Eser, S., Mathews, J., Yang, M.-gang, Jones, D., 2003. Molecular Size of Asphaltene Solubility Fractions. Energy & Fuels 44, 498-503.

51. Gutiérrez, L.B., Ranaudo, M.A., Méndez, B., Acevedo, S., 2001. Fractionation of Asphaltene by Complex Formation with p -Nitrophenol. A Method for Structural Studies and Stability of Asphaltene Colloids. Energy & Fuels 15, 624-628.

52. Hildebrand, J.H., 1919. SOLUBILITY. III. RELATIVE VALUES OF INTERNAL PRESSURES AND THEIR PRACTICAL APPLICATION. Journal of the American Chemical Society 41, 1067-1080.

53. Hildebrand, J.H., Prausnitz, J.M., Scott, R.L., 1970. Regular and related solutions: the solubility of gases, liquids, and solids. Van Nostrand Reinhold Co.

54. Hughey, C. a, Rodgers, R.P., Marshall, A.G., 2002. Resolution of 11,000 compositionally distinct components in a single electrospray ionization Fourier transform ion cyclotron resonance mass spectrum of crude oil. Analytical chemistry 74, 4145-9.

55. Hwang, T.L., Shaka, A.J., 1992a. Reliable Two-Dimensional Rotating-Frame Cross-Relaxation Measurements in Coupled Spin Systems. Journal of Magnetic Resonance, Series B 102, 155–165.

56. Hwang, T.L., Shaka, A.J., 1992b. Cross Relaxation without TOCSY: Transverse Rotating-Frame Overhauser Effect Spectroscopy. Journal of the American Chemical Society 114, 3157-3159.

57. Ignasiak, T., Kemp-Jones, A.V., Strausz, O.P., 1977. The molecular structure of Athabasca asphaltene. Cleavage of the carbon-sulfur bonds by radical ion electron transfer reactions. The Journal of Organic Chemistry 42, 312-320.

58. Ito, S., Wehmeier, M., Brand, J., Kubel, C., Epsch, R., Rabe, J., Mullen, K., 2000. Synthesis and self-assembly of functionalized hexa-peri-hexabenzocoronenes . Chemistry - A European Journal 6, 4327-4342.

59. Jagtap, R.N., Ambre, A.H., 2005. Overview literature on matrix assisted laser desorption ionization mass spectroscopy (MALDI MS): basics and its applications in characterizing polymeric materials. BULLETIN OF MATERIALS SCIENCE 28, 515–528.

60. Johnson, C.S., 1999. Diffusion ordered nuclear magnetic resonance spectroscopy: principles and applications. Progress in Nuclear Magnetic Resonance Spectroscopy 34, 203-256.

61. Karimi, A., Qian, K., Olmstead, W.N., Freund, H., Yung, C., Gray, M.R., 2011. Quantitative Evidence for Bridged Structures in Asphaltenes by Thin Film Pyrolysis. Energy & Fuels 25, 3581-3589.

62. Kastler, M., Pisula, W., Wasserfallen, D., Pakula, T., Müllen, K., 2005. Influence of alkyl substituents on the solution- and surface-organization of hexa-peri-hexabenzocoronenes. Journal of the American Chemical Society 127, 4286–96.

63. Khvostichenko, D.S., Andersen, S.I., 2008. Interactions between Asphaltenes and Water in Solutions in Toluene. Energy & Fuels 22, 3096-3103.

64. Kumar, K., Nikolov, A.D., Wasan, D.T., 2001. Mechanisms of Stabilization of Water-in-Crude Oil Emulsions. Industrial & Engineering Chemistry Research 40, 3009-3014.

65. Levitt, M.H., 2008. Spin Dynamics: Basics of Nuclear Magnetic Resonance. John Wiley & Sons.

66. Luo, R.-S., Mao, X.-A., 1997. Observation of the exchange of small molecules between phases in a SDS micellar system. Chemical Physics Letters 270, 77–80.

67. Martin, R.B., 1996. Comparisons of Indefinite Self-Association Models. Chemical reviews 96, 3043–3064.

68. Merdrignac, I., Quoineaud, A.-A., Gauthier, T., 2006. Evolution of Asphaltene Structure during Hydroconversion Conditions. Energy & Fuels 20, 2028-2036.

69. Merino-Garcia, D., Andersen, S.I., 2003. Isothermal Titration Calorimetry and Fluorescence Spectroscopy Study of Asphaltene Self-Association in

Toluene and Interaction with a Model Resin. Petroleum Science and Technology 21, 507-525.

70. Merino-Garcia, D., Andersen, S.I., 2004. Interaction of Asphaltenes with Nonylphenol by Microcalorimetry. Langmuir 20, 1473-1480.

71. Mitchell, D.L., Speight, J.G., 1973. The solubility of asphaltenes in hydrocarbon solvents. Fuel 52, 149-152.

72. Morris, K.F., Johnson, C.S., 1992. Diffusion-ordered two-dimensional nuclear magnetic resonance spectroscopy. Journal of the American Chemical Society 114, 3139-3141.

73. Mullins, O.C., 2010. The Modified Yen Model. Energy & Fuels 24, 2179-2207.

74. Mullins, O.C., Martínez-Haya, B., Marshall, A.G., 2008. Contrasting Perspective on Asphaltene Molecular Weight. This Comment vs the Overview of A. A. Herod, K. D. Bartle, and R. Kandiyoti. Energy & Fuels 22, 1765-1773.

75. Murgich, J., 2003. Molecular Simulation and the Aggregation of the Heavy Fractions in Crude Oils. Molecular Simulation 29, 451-461.

76. Murgich, J., Aray, Y., 1996. Molecular Recognition and Molecular Mechanics of Micelles of Some Model Asphaltenes and Resins. Energy & Fuels 10, 68-76.

77. Pekerar, S., Lehmann, T., Méndez, B., Acevedo, S., 1999. Mobility of Asphaltene Samples Studied by 13 C NMR Spectroscopy. Energy & Fuels 13, 305-308.

78. Pelet, R., Behar, F., Monin, J.C., 1986. Resins and asphaltenes in the generation and migration of petroleum. Organic Geochemistry 10, 481-498.

79. Pfeiffer, J.P., Saal, R.N.J., 1940. Asphaltic bitumen as colloid system. The Journal of Physical Chemistry 44, 139-165.

80. Pierre, C., Barré, L., Pina, A., Moan, M., 2004. Composition and Heavy Oil Rheology. Oil & Gas Science and Technology 59, 489-501.

81. Qian, K., Edwards, K.E., Siskin, M., Olmstead, W.N., Mennito, A.S., Dechert, G.J., Hoosain, N.E., 2007. Desorption and Ionization of Heavy Petroleum Molecules and Measurement of Molecular Weight Distributions. Energy & Fuels 21, 1042-1047.

82. Rakotondradany, F., Fenniri, H., Rahimi, P., Gawrys, K.L., Kilpatrick, P.K., Gray, M.R., 2006. Hexabenzocoronene Model Compounds for Asphaltene Fractions: Synthesis & Characterization. Energy & Fuels 20, 2439-2447.

83. Rubinstein, I., Spyckerelle, C., Strausz, O.P., 1979. Pyrolysis of asphaltenes: a source of geochemical information. Geochimica et Cosmochimica Acta 43, 1-6.

84. Rubinstein, I., Strausz, O.P., 1979. Thermal treatment of the Athabasca oil sand bitumen and its component parts. Geochimica et Cosmochimica Acta 43, 1887-1893.

85. Ruelle, P., Buchmann, M., Nam-Tran, H., Kesselring, U.W., 1992. Enhancement of the solubilities of polycyclic aromatic hydrocarbons by

weak hydrogen bonds with water. Journal of computer-aided molecular design 6, 431–48.

86. Samanta, U.., Chakrabarti, P.., Chandrasekhar, J.., 1998. Ab Initio Study of Energetics of X-H ,,, π (X) N , O , and C) Interactions Involving a. The Journal of Physical Chemistry A 8964–8969.

87. Sanna, C., La Mesa, C., Mannina, L., Stano, P., Viel, S., Segre, A., 2006. New class of aggregates in aqueous solution: an NMR, thermodynamic, and dynamic light scattering study. Langmuir : the ACS journal of surfaces and colloids 22, 6031–41.

88. Seidl, P., Chrisman, E., Silva, R., de Menezes, S., Teixeira, M., 2004. Critical variables for the characterization of asphaltenes extracted from vacuum residues . PETROLEUM SCIENCE AND TECHNOLOGY 22, 961-971.

89. Shaw, J.M., Zou, X., 2007. Phase Behavior of Heavy Oils. Asphaltenes, Heavy Oils, and Petroleomics 489-510.

90. Sheremata, J.M., Gray, M.R., Dettman, H.D., Mccaffrey, W.C., 2004. Quantitative Molecular Representation and Sequential Optimization of Athabasca Asphaltenes. Energy & Fuels 18, 1377-1384.

91. Shetty, A.S., Fischer, P.R., Stork, K.F., Bohn, P.W., Moore, J.S., 1996. Assembly of Amphiphilic Phenylacetylene Macrocycles at the Air−Water Interface and on Solid Surfaces. Journal of the American Chemical Society 118, 9409–9414.

92. Shetty, A.S., Zhang, J., Moore, J.S., 1996. Aromatic π-Stacking in Solution as Revealed through the Aggregation of Phenylacetylene Macrocycles. Journal of the American Chemical Society 118, 1019–1027.

93. Sheu, E.Y., 2002. Petroleum AsphalteneProperties, Characterization, and Issues. Energy & Fuels 16, 74-82.

94. Sheu, E.Y., Liang, K.., Sinha, S.., Overfield, R.., 1992. Polydispersity analysis of asphaltene solutions in toluene. Journal of Colloid and Interface Science 153, 399-410.

95. Siskin, M., Kelemen, S.R., Eppig, C.P., Brown, L.D., Afeworki, M., 2006. Asphaltene Molecular Structure and Chemical Influences on the Morphology of Coke Produced in Delayed Coking. Energy & Fuels 21, 2447-2454.

96. Speight, J.G., 2004. Petroleum Asphaltenes - Part 1: Asphaltenes, Resins and the Structure of Petroleum. Oil & Gas Science and Technology 59, 467-477.

97. Speight, J.G., 2006. The Chemistry and Technology of Petroleum, Fourth Edition. CRC Press.

98. Speight, J.G., 2007. The Chemistry and Technology of Petroleum FOURTH EDITION Preface.

99. Speight, J.G., Long, R.B., Trowbridge, T.D., 1984. Factors influencing the separation of asphaltenes from heavy petroleum feedstocks. Fuel 63, 616-620.

100. Spiecker, P.M., Gawrys, K.L., Kilpatrick, P.K., 2003. Aggregation and solubility behavior of asphaltenes and their subfractions. Journal of Colloid and Interface Science 267, 178-193.

101. Strausz, O.P., Lown, E.M., 2003. The Chemistry of Alberta Oil Sands, Bitumens and Heavy Oils . Alberta Energy Research Institute.

102. Strausz, O.P., Mojelsky, T.W., Lown, E.M., 1992. The molecular structure of asphaltene: an unfolding story. Fuel 71, 1355-1363.

103. Strausz, O.P., Peng, P., Murgich, J., 2002. About the Colloidal Nature of Asphaltenes and the MW of Covalent Monomeric Units. Energy & Fuels 16, 809-822.

104. Strausz, O.P., Safarik, I., Lown, E.M., 2008. A Critique of Asphaltene Fluorescence Decay and Depolarization-Based Claims about Molecular Weight and. Energy & Fuels 22, 1156-1166.

105. Tan, X., 2011. Personal communication.

106. Tan, X., Fenniri, H., Gray, M.R., 2008. Pyrene Derivatives of 2 , 2 ′ -Bipyridine as Models for Asphaltenes︰ Synthesis , Characterization , and Supramolecular Organization †. Energy & Fuels 715-720.

107. Tan, X., Fenniri, H., Gray, M.R., 2009. Water Enhances the Aggregation of Model Asphaltenes in Solution via Hydrogen Bonding. Energy & Fuels 9080-9086.

108. Tanaka, R., Hunt, J.E., Winans, R.E., Thiyagarajan, P., Sato, S., Takanohashi, T., 2003. Aggregates Structure Analysis of Petroleum

Asphaltenes with Small-Angle Neutron Scattering. Energy & Fuels 17, 127-134.

109.   Tchebotareva, N., Yin, X., Watson, M.D., Samorì, P., Rabe, J.P., Müllen, K., 2003. Ordered architectures of a soluble hexa-peri-hexabenzocoronene-pyrene dyad: thermotropic bulk properties and nanoscale phase segregation at surfaces. Journal of the American Chemical Society 125, 9734-9739.

110.   Varadaraj, R., Brons, C., 2007. Molecular Origins of Heavy Oil Interfacial Activity Part 1: Fundamental Interfacial Properties of Asphaltenes Derived from Heavy Crude Oils and Their Correlation To Chemical Composition. Energy & Fuels 21, 195-198.

111.   Wiehe, I.A., Jermansen, T.G., 2003. Design of Synthetic Dispersants for Asphaltenes. Petroleum Science and Technology 21, 527-536.

112.   Williams, D.B.G., Lawton, M., 2010. Drying of organic solvents: quantitative evaluation of the efficiency of several desiccants. The Journal of organic chemistry 75, 8351–4.

113.   Xing, C., Hilts, R.W., Shaw, J.M., 2010. Sorption of Athabasca Vacuum Residue Constituents on Synthetic Mineral and Process Equipment Surfaces from Mixtures with Pentane. Energy & Fuels 24, 2500-2513.

114.   Yan, Z., Elliott, J., Masliyah, J., 1999. Roles of Various Bitumen Components in the Stability of Water-in-Diluted-Bitumen Emulsions. Journal of colloid and interface science 220, 329–337.

115.   Yarranton, H.W., Alboudwarej, H., Jakher, R., 2000. Investigation of Asphaltene Association with Vapor Pressure Osmometry and Interfacial Tension Measurements. Industrial & Engineering Chemistry Research 39, 2916-2924.

116.   Yudin, I.K., Anisimov, M.A., 2007. Dynamic Light Scattering Monitoring of Asphaltene Aggregation in Crude Oils and Hydrocarbon Solutions. Asphaltenes, Heavy Oils, and Petroleomics 439-468.

117.   Zhang, L.Y., Breen, P., Xu, Z., Masliyah, J.H., 2007. Asphaltene Films at a Toluene / Water Interface. Energy & Fuels 274–285.

118.   Zhang, L.Y., Lopetinsky, R., Xu, Z., Masliyah, J.H., 2005. Asphaltene Monolayers at a Toluene / Water Interface. Energy & Fuels 256, 1330–1336.

119.   Zhang, L.Y., Xu, Z., Masliyah, J.H., 2005. Characterization of Adsorbed Athabasca Asphaltene Films at Solvent−Water Interfaces Using a Langmuir Interfacial Trough. Industrial & Engineering Chemistry Research 44, 1160-1174.

120.   di Primio R, Horsfield, B., Guzman-Vega, M., 2000. Determining the temperature of petroleum formation from the kinetic properties of petroleum asphaltenes. Nature 406, 173-6.